

Pareto Smoothed Importance Sampling*

Aki Vehtari[†] Daniel Simpson[‡] Andrew Gelman[§] Yuling Yao[§] Jonah Gabry[§]

2 July 2019

Abstract

Importance weighting is a general way to adjust Monte Carlo integration to account for draws from the wrong distribution, but the resulting estimate can be noisy when the importance ratios have a heavy right tail. This routinely occurs when there are aspects of the target distribution that are not well captured by the approximating distribution, in which case more stable estimates can be obtained by modifying extreme importance ratios. We present a new method for stabilizing importance weights using a generalized Pareto distribution fit to the upper tail of the distribution of the simulated importance ratios. The method, which empirically performs better than existing methods for stabilizing importance sampling estimates, includes stabilized effective sample size estimates, Monte Carlo error estimates and convergence diagnostics.

Keywords: importance sampling, Monte Carlo, Bayesian computation

1. Introduction

Importance sampling is a simple modification to the Monte Carlo method for computing expectations that is useful when there is an auxiliary distribution $g(\theta)$ that is easier to directly sample from than the target distribution $p(\theta)$, which may be only known up to a proportionality constant. The starting point is the simple Monte Carlo estimate for the expectation of a function h ,

$$I_h = E_p(h) = \int h(\theta)p(\theta) d\theta \approx \frac{1}{S} \sum_{s=1}^S h(\theta_s),$$

which requires exact draws θ_s , $s = 1, \dots, S$ from $p(\theta)$. The importance sampling estimate for the same expectation is

$$\frac{\sum_{s=1}^S r_s h(\theta_s)}{\sum_{s=1}^S r_s}, \quad r_s = \frac{f(\theta_s)}{g(\theta_s)}, \quad (1)$$

which only requires draws θ_s from a proposal distribution $g(\theta)$.

The success of the self-normalized importance sampling estimator depends on the distribution of importance ratios r_s . When the proposal distribution is a poor approximation to the target distribution, the distribution of importance ratios can have a heavy right tail. This can lead to unstable importance weighted estimates, sometimes with infinite variance.

The textbook examples of poorly performing importance samplers occur in low dimensions when the proposal distribution has lighter tails than the target, but it would be a mistake

*We thank Juho Piironen for help with R implementation, Tuomas Sivula for help with Python implementation, Viljami Aittomäki for help with protein expression data, Michael Riis Andersen and Srikanth Cadicherla for comments, and Academy of Finland, the Alfred P. Sloan Foundation, U.S. National Science Foundation, Institute for Education Sciences, the Office of Naval Research, the Natural Sciences and Engineering Research Council of Canada and the Canadian Research Chair programme for partial support of this research.

[†]Helsinki Institute for Information Technology HIIT, Department of Computer Science, Aalto University, Finland.

[‡]Department of Statistical Sciences, University of Toronto, Canada.

[§]Department of Statistics, Columbia University, New York.

to assume that heavy tailed proposals will stabilize importance samplers. This intuition is particularly misplaced in high dimensions, where importance sampling can fail even when the ratios have finite variance. MacKay (2003, Section 29.2) provides an example of what goes wrong in high dimensions: essentially, the ratios r_s will vary by several orders of magnitude and the estimator (1) will be dominated by a few draws. Hence, even if the approximating distribution is chosen so that the importance ratios are bounded and thus (1) has finite variance, the bound can be so high and the variance so large that the behaviour of the self-normalized importance sampling estimator is practically indistinguishable from an estimator with infinite variance. This suggests that if we want an importance sampling method that works in high dimensions, we need to move beyond being satisfied with estimates that have finite variance and towards methods with built-in error assessment.

In this paper, we propose the Pareto smoothed importance sampling (PSIS) method for stabilizing importance sampling estimates. As well as having the usual properties for a well-behaved self-normalized importance sampling estimator such as consistency, finite variance, and asymptotic normality, PSIS provides a simple numeric summary diagnostic that can be used to assess the method for a given sample, $(\theta_s)_{s=1}^S$. Beyond the examples in the latter part of this paper, PSIS forms the basis for the widely-used `loo` R package for stable, high-dimensional leave-one-out cross validation (Vehtari et al., 2017, 2018). This package has been downloaded more than 350 000 times.

2. Stabilizing importance sampling estimates by modifying the ratios

The stability of self-normalized importance sampling methods can be improved by directly modifying the computed ratios. For notational convenience, we rewrite these importance samplers as,

$$\int h(\theta)p(\theta) d\theta \approx \frac{\sum_{s=1}^S w_s h(\theta_s)}{\sum_{s=1}^S w_s}, \quad (2)$$

where $w_s = r_s$ would recover the standard self-normalized importance sampler.

Ionides (2008) showed that the truncation rule

$$w_s = \min\left(r_s, \sqrt{S\bar{r}}\right), \quad (3)$$

where \bar{r} is the average of the original S importance ratios, is consistent with finite variance and asymptotic normality. The critical advantage conveyed by the truncation is that these properties now extend to problems that only have integrable ratios; that is, we get asymptotic normality under the assumption that $\mathbb{E}(|r_s|) < \infty$ instead of under the stronger condition $\mathbb{E}(|r_s|^2) < \infty$ which is needed for the unmodified importance sampling estimator (1) to have finite variance.

This simple modification to the raw importance ratio greatly extends the range of problems for which the estimator has finite variance and asymptotic normality. Unfortunately, while the truncation can improve the stability of the weights, our experiments show that the simple weight modification scheme can be too severe, leading to larger than necessary finite sample bias.

2.1. Modeling the tail of the importance ratios

In this paper we propose a new scheme for modifying the extreme importance ratios that adapts more readily to the problem under consideration than the universal truncation rule of Ionides (2008).

To motivate the new scheme, we begin by noting that the success of plain importance sampling depends entirely on how many moments the importance ratios r_s possess, with the estimator having finite variance if the importance weights have finite variance. Chen and Shao (2004) and Koopman et al. (2009) show that when the importance ratios have more than two finite moments, the convergence rate of the estimators improves. This suggests that using information about the distribution of $r_s|r_s > u$, for some threshold $u \rightarrow \infty$ as $S \rightarrow \infty$, should allow us to improve the quality of our importance sampling estimators.

Pickands (1975) proved, under commonly satisfied conditions, that as sample size increases the distribution of $r_s|r_s > u$ is well approximated by the three-parameter generalized Pareto distribution,

$$p(y|u, \sigma, k) = \begin{cases} \frac{1}{\sigma} \left(1 + k \left(\frac{y-u}{\sigma}\right)\right)^{-\frac{1}{k}-1}, & k \neq 0 \\ \frac{1}{\sigma} \exp\left(-\frac{y-u}{\sigma}\right), & k = 0, \end{cases} \quad (4)$$

where u is a lower bound parameter, y is restricted to the range (u, ∞) , σ is a non-negative scale parameter, and k is an unconstrained shape parameter. The generalized Pareto distribution has $\lfloor 1/k \rfloor$ finite moments when $k > 0$, and thus we can infer the number of existing moments of the weight distribution by focusing on k .

To estimate the parameters in the generalized Pareto distribution, we use the M largest importance ratios, where

$$M = \begin{cases} 3\sqrt{S}, & S > 225, \\ S/5, & S \leq 225. \end{cases}$$

Restricting the tail modeling to a subset of the largest importance ratios implicitly defines a value of u in the Pareto distribution. The above choice of M was made based on extensive computational theory and in line with the requirements for consistent estimation (Pickands, 1975). In practice, we have found that the method is mostly indifferent to the exact form of M ; for instance, using $M = S/5$ in all cases was suggested by Vehtari et al. (2017) and it worked well even though it is not asymptotically correct. We tested several other methods (Scarrot and MacDonald, 2012) for selecting u directly, but found them to be more noisy than this simple heuristic.

The scale and shape parameters, σ and k , can be estimated using the highly efficient, low-bias method of Zhang and Stephens (2009). We chose this approach due to its efficiency and its ability to be used automatically without human intervention. In Appendix C we describe additional practical regularization of \hat{k} , which helps to reduce the variance of the estimate when S is small, without affecting the asymptotic properties.

Occasionally, we will use a h -specific tail estimate \hat{k}_h for the tail of the distribution $h(\theta)r(\theta)$, $\theta \sim g(\theta)$. This can be useful when $h(\theta)$ is unbounded or goes to zero, as it is possible if h grows fast enough (or goes to zero fast enough) relative to $r(\theta)$ that the tail behavior of $r(\theta)h(\theta)$ can be qualitatively different to the tail behavior of $r(\theta)$.

Although in most cases we cannot verify that the distribution of r_s lies in the domain of attraction for an extremal distribution, we will use this as a working assumption for building our method. Pickands (1975) notes that “most ‘textbook’ continuous distribution functions” (Gumbel, 1958) lie in the domain of attraction of some extremal distribution function. For finite S , we could alternatively interpret \hat{k} as saying that the sample $(r(\theta_s))_{s=1}^S$ is not statistically distinguishable from a sample of size S from a distribution with tail index \hat{k} .

Input: Raw importance ratios r_s , $s = 1, \dots, S$, ordered from highest to lowest

Output: PSIS-smoothed importance weights w_s , $s = 1, \dots, S$

Set $M = 3\sqrt{S}$ if $S > 225$, or $S/5$ if $S \leq 225$;

Set $w_s = r_s$, $s = 1, \dots, M - 1$;

Set $\hat{u} = r_M$;

Estimate $(\hat{k}, \hat{\sigma})$ in the generalized Pareto distribution from the M largest importance ratios, using the algorithm of Zhang and Stephens (2009) with the additional prior described in Appendix C;

Set $w_{M+z-1} = \min\left(F^{-1}\left(\frac{z-1/2}{M}\right), \max_s(r_s)\right)$, for each $z = 1, \dots, M$;

If the estimated shape parameter \hat{k} exceeds 0.7, report a warning that the resulting importance sampling estimates are likely to be unstable;

Algorithm 1: *The PSIS procedure for computing the importance weights.*

2.2. Our proposal: Pareto smoothed importance sampling

We propose a new method to stabilize the importance weights by replacing the M largest weights above the threshold u by a set of well-spaced values that are consistent with the tails of the importance distribution,

$$\begin{aligned} w_{M+z-1} &= F^{-1}\left(\frac{z-1/2}{M}\right) \\ &= r_{(S-M+1:S)} + k^{-1}\sigma \left[\left(1 - \frac{z-1/2}{M}\right)^{-k} - 1 \right] \\ &:= r_{(S-M:S)} + \tilde{w}_z, \end{aligned}$$

where $z = 1, \dots, M$, and F^{-1} is the inverse-CDF of the generalized Pareto distribution fitted to the M largest importance ratios.

The resulting Pareto smoothed importance sampler can be written as

$$I_h^S = \frac{1}{S} \sum_{s=1}^S (r(\theta_s) \wedge r_{(S-M+1:S)}) h(\theta_s) + \frac{1}{S} \sum_{m=1}^M \tilde{w}_m h(\theta_{S-M+m}).$$

This facilitates the view of PSIS as a generalization of truncated importance sampling with a problem-adapted threshold and a bias correction term. This estimator, summarized in Algorithm 1, is asymptotically consistent and has finite, vanishing variance under relatively light conditions. The final step in the algorithm warns the user if the estimated smoothness parameter in the generalized Pareto distribution is larger than 0.7. This is an automatic stability check that we justify using a complexity analysis in Section 3.

We recommend estimating the Monte Carlo error by formally adapting the estimator provided by Owen (2013, Ch. 9) for self-normalized importance sampling,

$$\widehat{\text{Var}}(\hat{I}_h^S) \approx \sum_{s=1}^S w_s^2 (h(\theta_s) - \tilde{\mu})^2.$$

If the draws have been obtained via MCMC, we recommend adjusting the above variance estimator to account for the autocorrelation in the sample,

$$\widehat{\text{Var}}(\hat{I}_h^S) \approx \sum_{s=1}^S w_s^2 (h(\theta_s) - \tilde{\mu})^2 / R_{\text{eff,MCMC}},$$

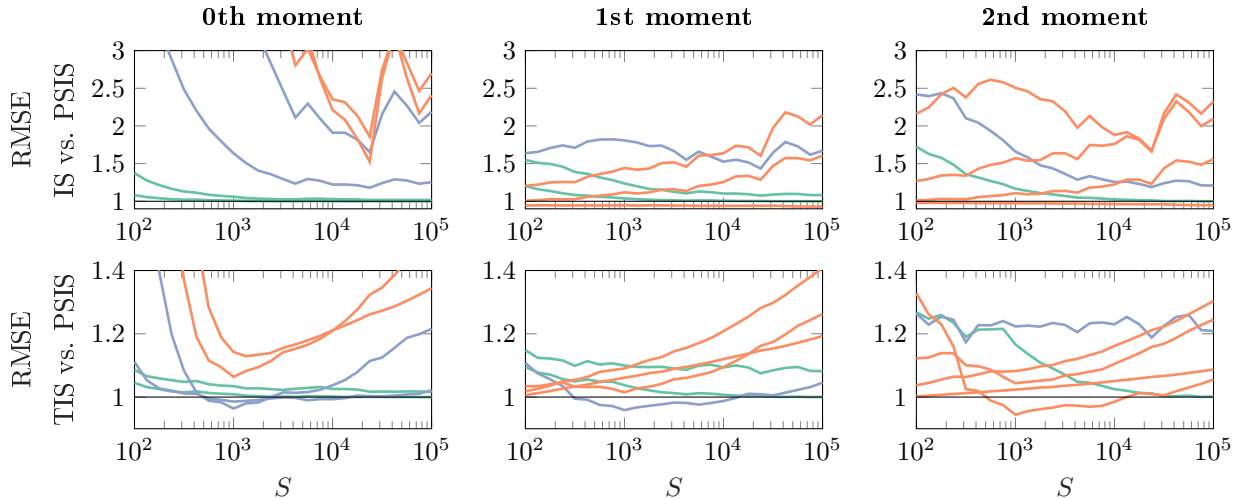


Figure 1: For Example 1, the ratio of root mean squared error between importance sampling (IS), truncated importance sampling (TIS), and Pareto smoothed importance sampling (PSIS) for $h(\theta) = 1$, $h(\theta) = \theta$, and $h(\theta) = \theta^2$. A ratio greater than 1 means PSIS had lower RMSE than its competitor. The target distribution is exponential(1) and the proposal distribution is exponential with rate (inverse mean) parameter $\theta \in (1.3, 1.5, 2, 3, 4, 10)$. The lines are colored according to the \hat{k}_h estimate. Green lines have $\hat{k}_h < 0.5$, blue lines have $0.5 < \hat{k}_h < 0.7$, and red lines have $\hat{k}_h > 0.7$.

where $R_{\text{eff,MCMC}} = S_{\text{eff,MCMC}}/S$ is the relative efficiency of MCMC, and the effective sample size $S_{\text{eff,MCMC}}$ for $h(\theta)$ is computed using the split-chain effective sample size estimate method (Vehtari et al., 2019). We validate these approximations using the examples in Appendix B.

The following example shows how PSIS compares with straight importance sampling and truncated importance sampling for a simple one dimensional example. Further simulated examples in low and moderate dimensions can be found in Appendix B.

Example 1. Consider the following one-dimensional example where the target distribution is exponential(1) and the proposal distributions are exponential(θ) for $\theta \in (1.3, 1.5, 2, 3, 4, 10)$, where the exponential is parameterized by the rate (inverse mean) parameter θ . The importance ratios will have infinite variance whenever $\theta > 2$ (Robert and Casella, 2004).

Figure 1 shows the ratio of root mean square errors (RMSEs) comparing ordinary, truncated, and Pareto smoothed importance sampling. In all cases a ratio larger than 1 corresponds to PSIS having the lower RMSE. It is clear that PSIS is always better than straight IS. On the other hand, PSIS is slightly worse than TIS with intermediate sample sizes for $\theta = 2$, which corresponds to $\hat{k} \approx 0.5$. A likely reason for this is that in this case the truncation rule in TIS is perfectly calibrated for the weight distribution and hence it is the best possible scenario for TIS. Deviations from this scenario lead to PSIS performing better. This is the only example we found where TIS outperformed PSIS. Figure 9 in Appendix B shows the distribution of the weights and estimates over several runs for this example when $\theta = 3$. From this, we see that PSIS yielded smaller bias but slightly larger variance than TIS. We further explore this example in Appendix B.1.

3. Using \hat{k} as a diagnostic

As part of the PSIS procedure, we estimate the shape parameter k of the limiting generalized Pareto distribution for the upper tail of the importance ratios. A simple option would be to

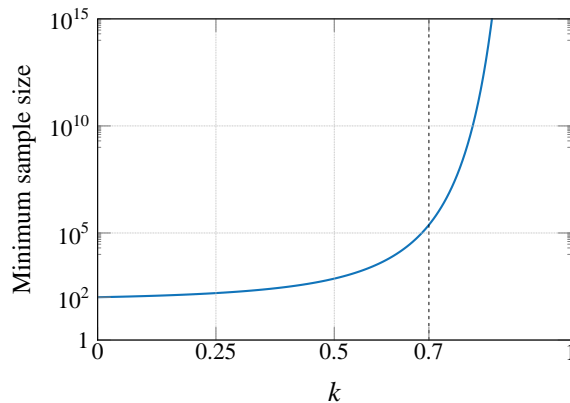


Figure 2: *Minimum sample size required as a function of k , as computed according to the heuristic (5). The required sample size quickly grows infeasibly large when $k > 0.7$.*

use this estimate \hat{k} and trust importance sampling as reliable if $\hat{k} \leq 0.5$. Our theory shows, however, that PSIS leads to valid and well-behaved importance sampling routines for any integrable density. This suggests that requiring the estimated shape parameter be less than 0.5 will be unnecessarily stringent.

Extensive experiments show that PSIS gives reliable (that is, low-bias, low variance) estimators of I_h when $\hat{k} < 0.7$. This can be interpreted as the estimate being reliable when the sample used to compute the PSIS estimate is indistinguishable from one that comes from a density with more than $0.7^{-1} = 1.43$ finite moments. When $\hat{k} > 0.7$ the convergence of the estimator becomes too slow to be useful.

In this section, we make the distinction between the true, but unknown, k and our finite sample estimate \hat{k} as a way to understand the differences between the asymptotic behaviour of PSIS and its finite sample behaviour. We first show theoretically that the computational complexity of importance sampling has a meaningful qualitative change around $k = 0.7$. We then demonstrate that the finite sample estimate \hat{k} is a useful indicator of the practical convergence of PSIS even when the distribution of ratios has finite variance. In particular, we show that \hat{k} can identify poorly behaved but finite variance proposals in high dimensions.

3.1. PSIS is reliable when $k < 0.7$

Several authors (Sanz-Alonso, 2018; Agapiou et al., 2017; Chatterjee and Diaconis, 2018), have proved, under a variety of assumptions, that a minimum sample size to control the importance sampling error is roughly

$$S \propto \exp(\text{KL}(p||g)) = \exp\left(\int p(\theta) \log\left(\frac{g(\theta)}{p(\theta)}\right) d\theta\right).$$

The most comprehensive results are due to Chatterjee and Diaconis (2018), who show that a larger sample size than this gives tail guarantees for the error in self-normalized importance sampling, while for smaller sample sizes it is not possible to control the large deviations. We can turn this theory into a heuristic bound by assuming that the density ratios $r(\theta) = p(\theta)/g(\theta)$ exactly form a Pareto distribution with shape parameter $k \in (0, 1)$ under g , in which case we can estimate $\text{KL}(p||g)$ by $\int_1^\infty r \log r \frac{1}{k} r^{-1/k-1} dr = k(1-k)^{-2}$. Hence, the minimal sample size,

$$S = \mathcal{O}\left(\exp\left(k(1-k)^{-2}\right)\right). \quad (5)$$

Figure 2 shows the estimated sample size as a function as k using the approximation (5). Although we do not recommend using this estimator directly due to both the uncertainty

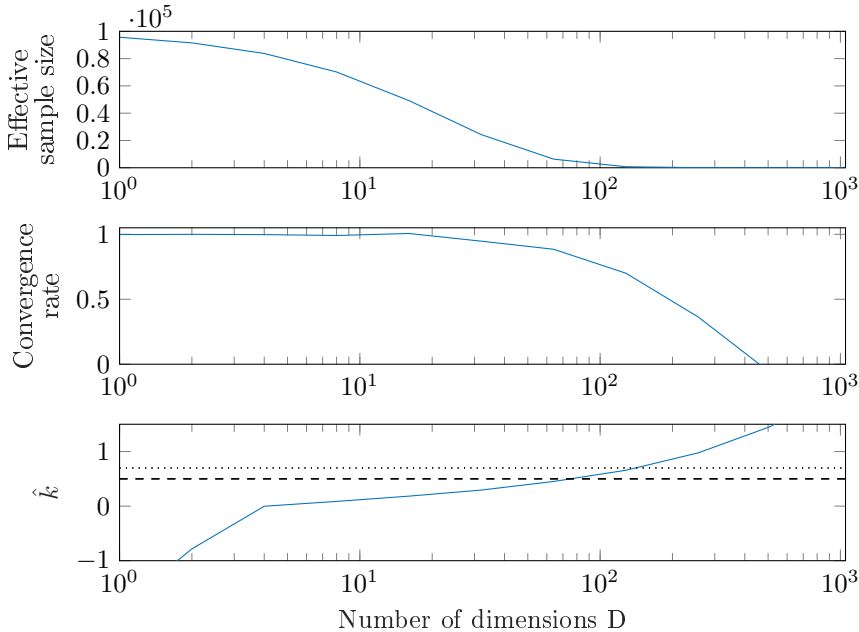


Figure 3: Top plot: *estimated effective sample size*. By $D = 64$, the 100 000 importance weighted draws have only a few practically non-zero weights. Middle plot: *convergence rate*. By $D = 128$ the convergence rate is about $S^{1/2}$, and getting any improvement in the accuracy becomes tedious. Bottom plot: \hat{k} diagnostic (dashed line at 0.5 and dotted line at 0.7) predicts well the observed convergence rate as discussed before.

in estimating k and the inaccuracy of the asymptotic approximation, we can see the quick increase in the order of magnitude for the minimum sample size around $k = 0.7$.

Although PSIS gives consistent, finite variance estimates when $k \in (0.7, 1)$, these complexity considerations suggest that they will not be practical in this regime. Simple experiments suggest that this type of behavior also holds for TIS, suggesting that the $k \approx 0.7$ may be a fundamental complexity barrier for useful importance sampling estimators.

3.2. \hat{k} is a good convergence diagnostic in finite samples and in high dimensions

Although importance sampling papers classically focus on the asymptotic properties of the estimator, the literature is full of examples where an importance sampling estimator is consistent, has finite variance, and is asymptotically normal but still fails to work. Most of these examples, such as the one in MacKay (2003, Sec. 29.2) where the importance ratios are bounded, occur in high dimensions. Hence, if we want PSIS to work reliably for problems of any dimension, we need to have a diagnostic that can flag poor convergence for any given sample of importance weights.

In the previous section, we argued that if we know the tail behaviour of the importance ratios, we can tell if PSIS will succeed within a reasonable computational budget. In this section, we argue that the estimate \hat{k} of the true tail index can quantify the finite sample behaviour. It does not matter what the actual tail behaviour is if the observed importance ratios “look” heavy tailed. In particular, we suggest the heuristic that if $\hat{k} > 0.7$, then the PSIS estimator will be unreliable.

The following example shows that \hat{k} can be an effective diagnostic for the real convergence behaviour. We see that the \hat{k} diagnostic correctly captures the collapse of the effective sample size (Owen, 2013, Section 9.3) and the convergence rate as the dimension increases.

Example 2. Let the target distribution be a D -dimensional normal with zero mean and identity covariance matrix, and let the proposal distribution be a multivariate Student- t with degrees of freedom $\nu = 7$ and with the same marginal variance as the target and a diagonal structure matrix. We take $S = 100\,000$ draws from the proposal distribution. Figure 3 shows what happens when the number of dimensions D ranges from 1 to 1024. Although the importance ratios are always bounded and the variance is finite, the finite sample behavior is indistinguishable from the infinite variance case when the number of dimensions grows large enough. The effective sample size and convergence rates drop dramatically, but this can be diagnosed with Pareto \hat{k} diagnostic. In these cases, we have just not yet reached the asymptotic regime where the central limit theorem kicks in.

4. Asymptotic results

In this section we show that PSIS is asymptotically consistent and has finite variance under some mild, but complex conditions on the distribution R of the ratios $r(\theta_s)$. The complexity here, relative to the corresponding results for TIS, comes from the use of an upper intermediate order statistic in place of a deterministic sequence of truncation points.

We also show that the modified version of PSIS, where both tails of $h(\theta_s)r(\theta_s)$ are replaced with the corresponding quantiles of (possibly different) modeled generalized Pareto distributions is asymptotically normal.

In this section, we focus mostly on the case where $k > 1/2$. The same results follow from identical arguments when $k \leq 1/2$ using the relevant tail bounds. For simplicity, we also limit ourselves to ordinary PSIS, although the asymptotic properties transfer to self-normalized PSIS by the usual arguments.

Finally, we assume that the parameters k and σ in the generalized Pareto distribution are fixed and known. We do not assume they are equal to the correct value, but we do not analyze their dependence on the sample of importance ratios.

4.1. Notation: Order statistics and concomitants

For the purpose of this section, we will take $M = \sqrt{S}$, which we will assume to be an integer. (Asymptotically, there is no difference between this and taking $M = \lfloor \sqrt{S} \rfloor$, however the notation gets messy.) Consider the order statistics $r_{1:S} \leq r_{2:S} \leq \dots \leq r_{S:S}$ of $r(\theta_k)$ and for convenience we will reorder the sample so that $r(\theta_s) = r_{s:S}$. It is also convenient to rewrite the weights on the upper tail as

$$w_j = F_S^{-1} \left(\frac{j - 1/2}{M} \right) = r_{(S-M+1):S} + k^{-1} \sigma \left[\left(1 - \frac{j - 1/2}{M} \right)^{-k} - 1 \right] := r_{(S-M+1):S} + \tilde{w}_j,$$

where \tilde{w}_j are deterministic (given k and σ) and $j = 1, \dots, M$.

We can then write the PSIS estimator as a randomized version of the truncated estimator of Ionides (2008) with an extra ‘‘bias correction’’ term

$$I_h^S = \frac{1}{S} \sum_{s=1}^S (r(\theta_s) \wedge r_{(S-M+1):S}) h(\theta_s) + \frac{1}{S} \sum_{j=1}^M \tilde{w}_j h(\theta_{S-M+j}).$$

Most of the complexity in the asymptotic results occur when $h(\theta)$ is unbounded. Because the Pareto smoothing only smoothes the ratios, it is possible that an unbounded $h(\theta)$ could still either break consistency or blow up the variance. Hence we need to investigate the properties of the concomitants $(r(\theta_s), h(\theta_s))$; David and Nagaraja (2003).

The relevant conditions on $h(\theta)$ will be stated in terms of the conditional expectations,

$$m_k(r) = \mathbb{E}_{\theta \sim g} (|h(\theta)|^k \mid r(\theta) = r).$$

In general, if we define the set $A_r = \{\theta : r(\theta) = r\}$, then

$$m_k(r) = \mathbb{E}_{\theta \sim g} (|h(\theta)|^k \mid \theta \in A_r).$$

We need to control $m_1(r)$ and $m_2(r)$, which basically corresponds to $h(\theta)$ not growing too fast and not varying too much on A_r as $r \rightarrow \infty$.

The following example shows that, in most cases, $m_k(r)$ will grow *very* slowly as a function of r . In particular, if $r(\theta)$ grows fast enough to have infinite variance under g , then $h(\theta)$ would have to grow faster than a polynomial for $m_k(r)$ to grow polynomially.

Example 3. *If both $h(\cdot)$ and $r(\cdot)$ are radially symmetric then $m_1(r)$ is a deterministic function. For example, if $h(\theta) = |\theta|^\ell$ and $r(\theta) = \exp(|\theta|^p)$, then, solving for $|\theta|$, we see that $h(r) = (\log(r))^{\ell/p}$ and hence $m_k(r) = (\log(r))^{k\ell/p}$.*

4.2. PSIS is asymptotically unbiased

With this in place, we can now state the following results, which are proved in the appendix. For simplicity we will only consider the case where the support of R is $[0, \infty)$. The arguments can be modified to account for finite right endpoints with minimal effort. We also assume that R has no atoms, which is reasonable in this context. The argument still holds as long as R is continuous near infinity.

Theorem 1. *Fix $k < 1$, $\sigma > 0$, set $M = \lfloor \sqrt{S} \rfloor$, and recall that we have ordered θ_s so that $r_{s:S} = r(\theta_s)$. Let R be the cumulative distribution function of the ratios $r(\theta_s)$ and assume that $1 - R(z) \sim z^{-1/k'}$ as $z \rightarrow \infty$ for some $k' < 1$ that doesn't need to be equal to k . Assume the following:*

A1 *For large enough S , and for all $c > 0$ and $\epsilon > 0$*

$$\frac{1 - R(\xi_M \pm \epsilon)}{1 - R(\xi_M)} \leq 1 \mp cS^{-1/2}, \quad (6)$$

where $\xi_M = R^{-1}(1 - M/S) \rightarrow \infty$ as $S \rightarrow \infty$.

A2 *The function*

$$e(t) = \int_{r(\theta) > t} h(\theta) p(\theta) d\theta$$

is continuous and $e(t) \rightarrow 0$ as $t \rightarrow \infty$.

A3 $\mathbb{E}(m_1(r_{S-M+1:S})r_{S-M+1:S}) = o(S)$

A4 $\mathbb{E}_g(|h(\theta)|) < \infty$.

Then the PSIS estimator is asymptotically unbiased. Furthermore, if $h(\theta)$ is a bounded function, then only (A1)–(A2) are required for the conclusion to hold.

The requirement that R has a generalized Pareto-like tail is critical to our method and, by standard extremes arguments, usually holds. Obvious modifications to the proof can be made when R limits to a different part of the generalized Pareto family. We have further assumed

that R has at least one moment, which is necessary for our self-normalized estimators to make sense.

The first two conditions are moderately mild. (A1) ensures that the quantile CDF does not have large jumps out near infinity. This type of condition will repeat in the next two sections. It is used to ensure that nothing too exciting happens beyond the truncation point and we expect it to be usually satisfied.

Similarly, (A2) requires that nothing interesting happens out in the tails of the integral. This condition holds if $h(\theta)$ and $p(\theta)$ are continuous functions. Assuming continuity for all t simplifies the argument, but noting that, for $S > 5$, $r_{s-M+1:S}$ has at least M finite moments (Sen, 1959), a similar result should hold if continuity holds for sufficiently large t through a Chebyshev-type argument.

When $h(\theta)$ is unbounded, we need some conditions on its growth relative to the growth of $r(\theta)$. Assumption (A3) is automatically satisfied if $m_1(r)$ grows at most polynomially (Sen, 1959). This assumption can be easily checked by regressing $h(\theta_s)$ against $r(\theta_s)$.

Assumption (A4) requires that $h(\cdot)$ is integrable with respect to the proposal distribution as well as target distribution. Although this isn't commonly required for importance sampling methods, it is usually satisfied, however if g has heavier tails than p , this will be a strictly stronger condition than the usual p -integrability.

4.3. The variance of PSIS is bounded and goes to zero

Next we show that, under some additional conditions, the PSIS estimate has finite variance.

Theorem 2. Fix $k > 1$, $\sigma > 0$, set $M = \lfloor \sqrt{S} \rfloor$, and recall that we have ordered θ_s so that $r_{s:S} = r(\theta_s)$. Let R be the cumulative distribution function of the ratios $r(\theta_s)$.

In addition to the conditions of Theorem 1, assume the following:

B1 R has $(1 + \delta)$ finite moments for some $\delta > 0$ and it satisfies the von Mises condition

$$\lim_{z \rightarrow \infty} \frac{z \tilde{r}(z)}{1 - R(z)} = \frac{1}{k'},$$

where \tilde{r} is the density of R and $k' < 1$, where k' is not necessarily the same as k .

B2 $\mathbb{E}(r_{S-M+1:S}^2(m_j(r_{S-M+1:S})) \vee 1) = o(S)$ uniformly $j = 1, 2$.

B3 $\mathbb{E}_g(h(\theta)^2) < \infty$.

Then the PSIS estimator has bounded variance that goes to zero as $S \rightarrow \infty$.

Condition (B1), which holds iff the density r is regularly varying at infinity with index k'^{-1} , is a standard condition to be able to estimate the tail-index of a generalized Pareto distribution. It ensures that $R|R > u$ is almost Pareto for large enough u , which is a fundamental assumption of our method (Falk and Marohn, 1993).

Condition (B2) is needed to control the tail values of $h(\theta)$ and the effect of the truncation parameter. It will hold assuming $h(\theta)$ doesn't vary wildly near infinity on level sets of $r(\cdot)$. This bound can be verified using the techniques in Rychlik (1994).

Condition (B3) requires that $h \in L^2(p) \cap L^2(g)$, which is potentially a stronger condition than the usual requirement that $h \in L^2(p)$ if g has heavier tails than p .

4.4. PSIS is asymptotically normal

In this section, we adapt the result of Griffin (1988) to show that a variant of PSIS is asymptotically normal. Rather than applying Pareto smoothing only to the ratios, in this section, we propose applying Pareto smoothing to the ratios $h(\theta_s)r(\theta_s)$. If h is unbounded both above and below, we need to Pareto smooth both ends of the sequence. With that in mind, let (σ_L, k_L) be the generalized Pareto parameters for the smallest M values of $h(\theta_s)r(\theta_s)$ and let (σ_R, k_R) be the generalized Pareto parameters for the M largest values of $h(\theta_s)r(\theta_s)$. Then, if we order the sample so $h(\theta_s)r(\theta_s) \leq h(\theta_t)r(\theta_t)$ whenever $s < t$, we get the modified PSIS estimator,

$$\begin{aligned} \tilde{I}_h^S &= \frac{1}{S} \sum_{s=M+1}^{S-M} h(\theta_s)r(\theta_s) + \frac{M}{S} h(\theta_M)r(\theta_M) + \frac{M}{S} h(\theta_{S-M+1})r(\theta_{S-M+1}) \\ &\quad + \frac{1}{S} \sum_{j=1}^M \left(k_R^{-1} \sigma_R \left[\left(1 - \frac{j-1/2}{M} \right)^{-k_R} - 1 \right] - k_L^{-1} \sigma_L \left[\left(\frac{j-1/2}{M} \right)^{-k_L} - 1 \right] \right). \end{aligned}$$

The following result is an application of the main result of Griffin (1988) to this estimator.

Theorem 3. *Let $F(\cdot)$ be the CDF of $h(\theta)r(\theta)$, $\theta \sim g$. Assume $R(z)$ is convex in some neighbourhood of $z = -\infty$ and $1 - R(z)$ in some neighbourhood of $z = \infty$ and that*

$$\lim_{z \rightarrow -\infty} \frac{|z|f(z)}{F(z)} = \frac{1}{k'_L}, \quad \lim_{z \rightarrow \infty} \frac{zf(z)}{1 - F(z)} = \frac{1}{k'_R},$$

for $0 < k_L, k_R < 1$, where $f(\cdot)$ is the density of F . Then there exists a sequence γ_S such that

$$c_S(\tilde{I}_h^S - I_h) \xrightarrow{d} N(0, \sigma^2),$$

where $c_S = \mathcal{O}(S^{1/2 \wedge (3/4 - k'/2)})$, where $k' = k'_L \vee k'_R$.

The assumption that F is convex at infinity can be dropped, at the cost of a less explicit form for the norming sequence (Griffin, 1988). The result also holds for more general trimming sequences and, if h is bounded below, then only the right hand tail is needed in the estimator.

5. Practical examples

In this section we present three examples where Pareto smoothed importance sampling improves the estimates and where the Pareto shape estimate \hat{k} is a useful diagnostic. In the first example PSIS is used to improve the distributional approximation (split-normal) of the posterior of a logistic Gaussian process density estimation model. We then demonstrate the performance and reliability of PSIS for leave-one-out (LOO) cross-validation analysis of Bayesian predictive models for the canonical stacks data as well as for a recent breast cancer tumor dataset with 105 different protein expressions. Further examples with simulated data can be found in Appendix B.

5.1. Improving distributional posterior approximation with importance sampling

The first example shows that PSIS can be useful for performing approximate Bayesian inference. PSIS has been used to stabilize expectation propagation-like algorithms Weber et al. (2016) as well as to improve and diagnose variational approximations to posteriors Yao

et al. (2018); Magnusson et al. (2019). In this section, we show that PSIS can be used to speed up logistic Gaussian process (LGP) density estimation (Riihimäki and Vehtari, 2014), which is implemented in the GPstuff toolbox (Vanhatalo et al., 2013); code available at <https://github.com/gstuff-dev/gpstuff>.

LGP provides a flexible way to define the smoothness properties of density estimates via the prior covariance structure, but the computation is analytically intractable. Riihimäki and Vehtari (2014) propose a fast computation using discretization of the normalization term and Laplace’s method for integration over the latent values.

Given n independently drawn d -dimensional data points x_1, \dots, x_n from an unknown distribution in a finite region (having a compact support) $\mathcal{V} \subset \mathbb{R}^d$, we want to estimate the density $p(x)$. To introduce the constraints that the density is non-negative and that its integral over \mathcal{V} is equal to 1, Riihimäki and Vehtari (2014) employ the logistic density transform,

$$p(x) = \frac{\exp(f(x))}{\int_{\mathcal{V}} \exp(f(s)) ds}, \quad (7)$$

where f is an unconstrained latent function. To smooth the density estimates, a Gaussian process prior is set for f , which allows for assumptions about the smoothness properties of the unknown density p to be expressed via the covariance structure of the GP prior. To make the computations feasible \mathcal{V} is discretized into finite m subregions (or intervals if the problem is one-dimensional). Here we skip the details of the Laplace approximation and focus on the importance sampling.

Following Geweke (1989), Riihimäki and Vehtari (2014) use importance sampling with a multivariate split Gaussian density as an approximation. The approximation is based on the posterior mode and covariance, with the density adaptively scaled along principal component axes (in positive and negative directions separately) to better match the skewness of the target distribution; see also Villani and Larsson (2006). To further improve the performance, Riihimäki and Vehtari (2014) replace the discontinuous split Gaussian used by Geweke with a continuous version.

Riihimäki and Vehtari (2014) use an ad hoc soft thresholding of the importance weights if the estimated effective sample size as defined by Kong et al. (1994) is less than a specified threshold. The approach can be considered to be a soft version of truncated importance sampling, which Ionides (2008) also mentions as a possibility without further analysis. Here we propose to use PSIS to stabilize the weights.

We repeat the density estimation using the Galaxy data set¹ 1000 times with different random seeds. The model has 400 latent values, that is, the posterior is 400 dimensional, although due to a strong dependency imposed by the Gaussian process prior the effective dimensionality is smaller. Because of this it is sufficient that the split-normal is scaled only along the first 50 principal component axes. In order to compare to a baseline method, we implement the Markov chain Monte Carlo scheme described in Riihimäki and Vehtari (2014). Computation time for MCMC inference was about half an hour and computation time for split-normal with importance sampling was about 1.3s (laptop with Intel Core i5-4300U CPU @ 1.90GHz x 4).

Figure 4 compares the Kullback-Leibler divergence from the density estimate using MCMC to the density estimates using the split-normal approximation with and without the importance sampling correction. The shaded areas show the envelope of the KL-divergence from all 1000 runs. The variability of the plain split-normal approximation (purple) diminishes as the number of draws S increases, but the KL-divergence does not decrease. IS (yellow) has high variability. PSIS (blue) performs well, with a small KL-divergence already when

¹<https://stat.ethz.ch/R-manual/R-devel/library/MASS/html/galaxies.html>

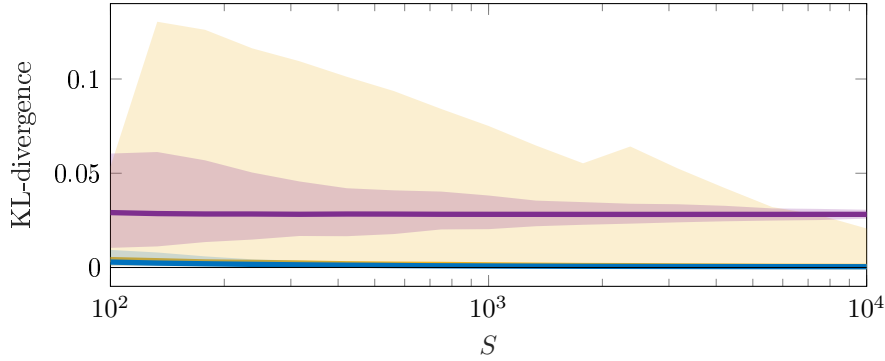


Figure 4: *Kullback-Leibler divergence from the density estimate using MCMC to the density estimates using the plain split-normal approximation (purple), IS (yellow), and PSIS (blue). The shaded areas show the envelope of the KL-divergence from all 1000 runs. The variability of plain split-normal approximation (purple) reduces with increasing number of draws S , but the KL-divergence doesn't decrease. IS (yellow) has high variability.*

S is only 100. TIS results (not shown) were mostly similar to PSIS, with some rare worse results (similar jumps as in Figure 21). The mean estimate for \hat{k} was 0.43 with $S = 100$ and 0.55 with $S = 10^4$, which explains the high variability of IS, the rare bad results from TIS, and the excellent performance of PSIS. These \hat{k} values also signal that we can trust the PSIS results.

The Pareto \hat{k} diagnostic can also be used to compare the quality of the distributional approximations. In the case of a simple normal approximation without split scaling, the mean \hat{k} with $S = 10^4$ was 0.60, and thus slightly higher variability and slower convergence can be assumed relative to the split-normal approximation.

5.2. Importance-sampling leave-one-out cross-validation

We next demonstrate the use of Pareto smoothed importance sampling for leave-one-out (LOO) cross-validation approximation. The i th leave-one-out cross-validation predictive density can be approximated with

$$p(\tilde{y}_i | y_{-i}) \approx \frac{\sum_{s=1}^S w_i(\theta^s) p(\tilde{y}_i | \theta^s)}{\sum_{s=1}^S w_i(\theta^s)}. \quad (8)$$

Importance sampling LOO was proposed by Gelfand et al. (1992), but for long time it was not widely used as the estimator is unreliable if the weights have infinite variance. For some simple models, such as linear and generalized linear models with specific priors, it is possible to analytically check the sufficient conditions for the variance of the importance weights in IS-LOO to be finite (Peruggia, 1997; Epifani et al., 2008), but this is not generally possible.

We first demonstrate properties of IS, TIS, and PSIS with the stack loss data, which is known to have one observation producing infinite variance for LOO importance ratios. Then we demonstrate the speed and reliability of PSIS-LOO for performing model assessment and comparison for predictive regression models for 105 different protein expressions.

LOO for stack loss data. The stack loss data has $n = 21$ daily observations on one response variable and three predictors pertaining to a plant for the oxidation of ammonia to nitric acid. The model is a simple Gaussian linear regression. We fit the model using Stan (Stan Development Team, 2017) (the code is in the appendix). Peruggia (1997) showed, for a

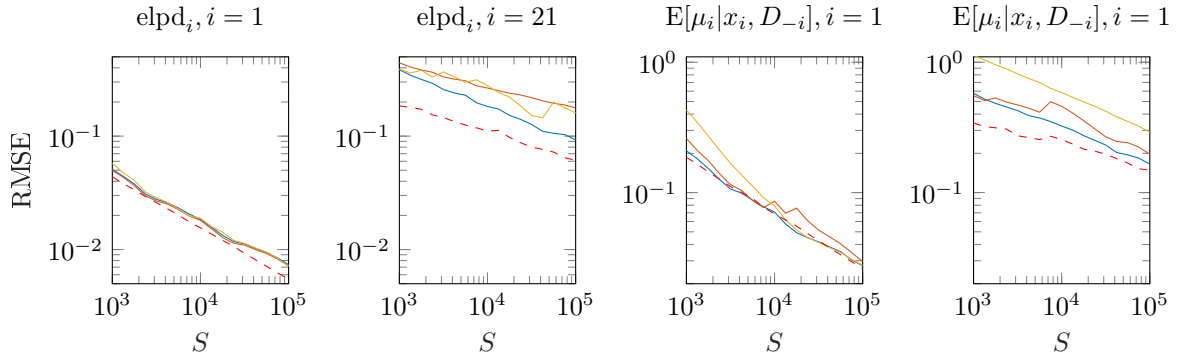


Figure 5: *RMSE with IS (yellow), TIS (red) and PSIS (blue), and the Monte Carlo error estimates with PSIS (red dashed) for the expected log predictive densities $\text{elpd}_i = \log p(y_i|x_i, D_{-i})$ and leave-one-out predictive mean $E[\mu_i|x_i, D_{-i}]$. Average h specific \hat{k} 's, using $S = 10^5$ draws from each of 100 runs, are 0.46, 0.79, 0.45, 0.81 (in the order of subplots).*

specific choice of prior distributions that we do not recommend using in real analyses, that the importance ratios have an infinite variance when leaving out the 21st data point.

Figure 5 shows the RMSE and Monte Carlo estimate from 100 runs for the LOO estimated expected log predictive densities $\text{elpd}_i = \log p(y_i|x_i, D_{-i})$ and leave-one-out predictive mean $E[\mu_i|x_i, D_{-i}]$ (where D_{-i} denotes the data without i th observation) estimated with IS, TIS and PSIS when leaving out the 1st or 21st observation. Pareto smoothing and Monte Carlo error estimates were adjusted based on relative MCMC sample efficiency. The true values were computed by actually leaving out the i th observation and using multiple long MCMC chains to get a small Monte Carlo error. We see that PSIS gives the smallest RMSE, and the accuracy of the Monte Carlo error estimates are what we would expect based on h specific \hat{k} 's (i.e., error estimates are accurate for $\hat{k} < 0.5$ and optimistic for $\hat{k} > 0.7$).

LOO for 105 protein expression data sets We demonstrate the benefit of fast importance sampling leave-one-out cross-validation and PSIS diagnostics with the example of a model for the combined effect of microRNA and mRNA expression on protein expression. The data were published by Aure et al. (2015) and are publicly available; we used the preprocessed data as described by Aittomäki (2016). Protein, mRNA, and microRNA expression were measured from 283 breast cancer tumor samples, and when predicting the protein expression the corresponding gene expression and 410 microRNA expressions were used. We assumed a multivariate linear model for the effects with a Gaussian prior and used Stan (Stan Development Team, 2017) to fit the model. Initial analyses gave reason to suspect outlier observations; to verify this we compared Gaussian and Student- t observations models.

For 4000 posterior draws, the computation for one gene and one model takes about 9 minutes (desktop Intel Xeon CPU E3-1231 v3 @ 3.40GHz x 8), which is reasonable speed. For all 105 genes the computation takes about 30 hours. Exact regular LOO for all models would take 125 days, and 10-fold cross-validation for all models would take about 5 days. Pareto smoothed importance sampling LOO (PSIS-LOO) took less than one minute for all models. However, we do get several leave-one-out cases where $\hat{k} > 0.7$, which we should not trust based on our results above. Figure 6 shows $\hat{k} > 0.7$ values for 105 Gaussian and Student- t linear models, where each model may have several leave-one-out cases with $\hat{k} > 0.7$. Large \hat{k} values arise when the proposal and the target distributions are very different, which is typical when there are highly influential observations. Switching to the Student- t model reduces the number of high \hat{k} values, as the outliers are less influential if they are far in

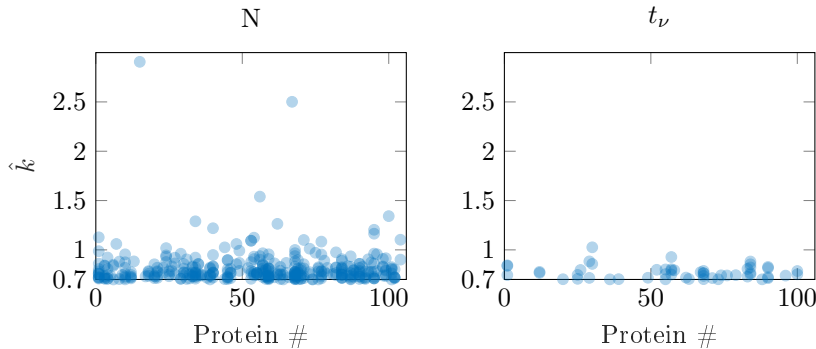


Figure 6: $\hat{k} > 0.7$ values for 105 Gaussian and Student- t linear models predicting protein expression levels.

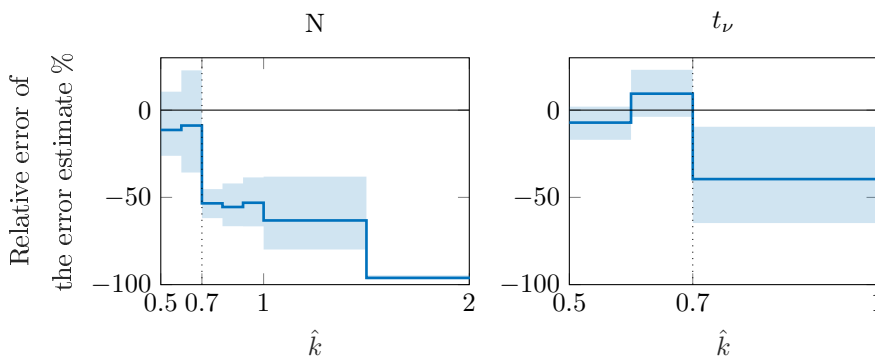


Figure 7: Relative error of the PSIS Monte Carlo error estimates. True error was computed as RMSE of expected log predictive density elpd_i estimates with \hat{k} on common interval (boundaries of intervals can be seen as steps in the plots).

the tail of the t -distribution. When working with many different models the Stan team has noticed that high \hat{k} values are also a useful indicator that there is something wrong with the data or the model (Gabry et al., 2019).

Figure 7 shows the accuracy of PSIS Monte Carlo error estimates for the expected log predictive densities with respect to different \hat{k} values (computed only for $\hat{k} > 0.5$). True values were computed by actually leaving out the i th observation and rerunning MCMC. We can see that \hat{k} is a useful diagnostic and the Monte Carlo error estimates are accurate for $\hat{k} < 0.7$, as in the simulation experiments, and fail for $\hat{k} \geq 0.7$.

To improve upon PSIS-LOO we can make the exact LOO computations for any points corresponding to $\hat{k} > 0.7$ (for which we cannot trust the Monte Carlo error estimates). In this example there were 352 such cases for the Gaussian models and 53 for the Student- t models, and the computation for these took 42 hours. Although combining PSIS-LOO with exact LOO for certain points substantially increases the computation time in this example, it is still less than the time required for 10-fold-CV.

The left subplot in figure 8 shows comparison of PSIS-LOO and PSIS-LOO+ (PSIS-LOO with exact computation for cases with $\hat{k} > 0.7$) when comparing the difference of expected log predictive densities $\sum_{i=1}^n (\text{elpd}_i(t_\nu) - \text{elpd}_i(N))$. We see that with high \hat{k} values, the error of PSIS-LOO can be large (the error would be large for IS and TIS, too). To trust the model comparison we recommended using PSIS-LOO+ with exact computation for cases with $\hat{k} > 0.7$ or K -fold-CV. The right subplot shows the final model comparison results for all 105

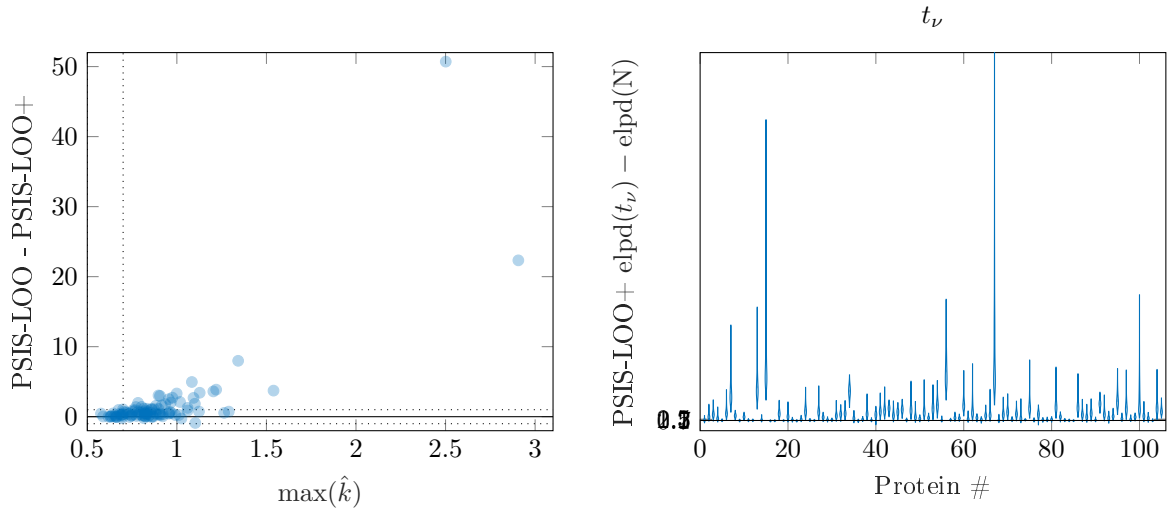


Figure 8: The left plot shows comparison of PSIS-LOO and PSIS-LOO+ (PSIS-LOO with exact computation for cases with $\hat{k} > 0.7$) when comparing the difference of expected log predictive densities $\sum_{i=1}^n (\text{elpd}_i(t_\nu) - \text{elpd}_i(N))$. The right plot shows the PSIS-LOO+ estimated improvement of expected log predictive densities when switching from Gaussian model to Student- t model.

models predicting protein expression levels. For most of the proteins, the student- t model is much better, and the Gaussian model is not significantly better for any of the proteins.

Paananen et al. (2019) present an iterative moment matching version of PSIS which is especially useful when MCMC has been used to sample from the proposal as is usual in PSIS-LOO. Bürkner et al. (2019) apply PSIS in leave-future-out cross-validation for time series, where the proposal distribution is conditioned on less data and thus by construction tend to have thicker tails than the target distribution, but with a large number of steps in time eventually new MCMC posterior computation is needed. Magnusson et al. (2019) apply PSIS-LOO in case of variational and Laplace approximations to posteriors.

6. Discussion

Importance weighting is a widely used tool in statistical computation. Even in the modern era of Markov chain Monte Carlo, approximate algorithms are often necessary, in which case we should adjust approximations when possible to better match target distributions. However, a challenge for practical applications of importance weighting is the well known fact that importance-weighted estimates are unstable if the weights have high variance.

In this paper we have shown that it is possible to reduce the mean square error of importance sampling estimates using a particular stabilizing transformation that we call Pareto smoothed importance sampling (PSIS). The key step is to replace the largest weights by expected quantiles from a generalized Pareto distribution. We have also demonstrated greatly improved Monte Carlo error estimates, natural diagnostics for gauging the reliability of the estimates, and empirical convergence rate results that closely follow known theoretical results.

The most important feature of PSIS is the \hat{k} diagnostic, which allows the user to assess the reliability of the estimator:

- If $k < \frac{1}{3}$ the Berry-Esseen theorem (Chen and Shao, 2004; Koopman et al., 2009) states

faster convergence rate to normality. If $\hat{k} < \frac{1}{3}$, we observe that importance sampling is stable and all IS, TIS and PSIS work well.

- If $k < \frac{1}{2}$ then the distribution of importance ratios has finite variance and the central limit theorem holds (Geweke, 1989). However the finite sample bias may still be quite large and the value of \hat{k} may be much larger than $1/2$ indicating that the importance sampler is unreliable for this realization of weights.
- If $\frac{1}{2} \leq k < 0.7$ then the variance is infinite and plain IS can behave quite poorly. However both TIS and PSIS work well in this regime.
- If $0.7 < k < 1$ it quickly becomes too expensive to get an accurate estimate. We do not recommend using importance sampling when $\hat{k} > 0.7$.
- If $k \geq 1$ then neither the variance nor the mean of raw ratios exists. The convergence rate is close to zero and bias can be large with practical sample sizes S .

With these recommendations, PSIS is a reliable, accurate, and trustworthy variant of important sampling that comes with a in-built heuristic that allows it to fail loudly when it becomes unreliable.

References

- Agapiou, S., Papaspiliopoulos, O., Sanz-Alonso, D., Stuart, A., et al. (2017). Importance sampling: Intrinsic dimension and computational cost. *Statistical Science*, 32(3):405–431.
- Aittomäki, V. (2016). MicroRNA regulation in breast cancer—a Bayesian analysis of expression data. Master’s thesis, Aalto University.
- Aure, M. R., Jernström, S., Krohn, M., Vollan, H. K., Due, E. U., Rødland, E., Kåresen, R., Ram, P., Lu, Y., Mills, G. B., Sahlberg, K. K., Børresen-Dale, A. L., Lingjærde, O. C., and Kristensen, V. N. (2015). Integrated analysis reveals microRNA networks coordinately expressed with key proteins in breast cancer. *Genome Medicine*, 7(1):21.
- Bürkner, P.-C., Gabry, J., and Vehtari, A. (2019). Approximate leave-future-out cross-validation for Bayesian time series models. *arXiv preprint 1902.06281*.
- Chatterjee, S. and Diaconis, P. (2018). The sample size required in importance sampling. *The Annals of Applied Probability*, 28(2):1099–1135.
- Chen, L. H. Y. and Shao, Q.-M. (2004). Normal approximation under local dependence. *The Annals of Probability*, 32(3):1985–2028.
- David, H. A. and Nagaraja, H. N. (2003). *Order Statistics*. John Wiley & Sons, Hoboken, New Jersey, third edition.
- Epifani, I., MacEachern, S. N., and Peruggia, M. (2008). Case-deletion importance sampling estimators: Central limit theorems and related results. *Electronic Journal of Statistics*, 2:774–806.
- Falk, M. and Marohn, F. (1993). Von Mises conditions revisited. *The Annals of Probability*, pages 1310–1328.

- Gabry, J., Simpson, D., Vehtari, A., Betancourt, M., and Gelman, A. (2019). Visualization in Bayesian workflow. *Journal of the Royal Statistical Society: Series A (Statistics in Society)*, 182(2):389–402.
- Gather, U. and Tomkins, J. (1995). On stability of intermediate order statistics. *Journal of statistical planning and inference*, 45(1-2):175–183.
- Gelfand, A. E., Dey, D. K., and Chang, H. (1992). Model determination using predictive distributions with implementation via sampling-based methods. In Bernardo, J. M., Berger, J. O., Dawid, A. P., and Smith, A. F. M., editors, *Bayesian Statistics 4*, pages 147–167. Oxford University Press.
- Geweke, J. (1989). Bayesian inference in econometric models using Monte Carlo integration. *Econometrica*, 57(6):1317–1339.
- Griffin, P. S. (1988). Asymptotic normality of Winsorized means. *Stochastic processes and their applications*, 29(1):107–127.
- Gumbel, E. J. (1958). *Statistics of Extremes*. Columbia University Press, New York.
- Ionides, E. L. (2008). Truncated importance sampling. *Journal of Computational and Graphical Statistics*, 17(2):295–311.
- Kong, A., Liu, J. S., and Wong, W. H. (1994). Sequential imputations and Bayesian missing data problems. *Journal of the American Statistical Association*, 89(425):278–288.
- Koopman, S. J., Shephard, N., and Creal, D. (2009). Testing the assumptions behind importance sampling. *Journal of Econometrics*, 149(1):2–11.
- MacKay, D. J. (2003). *Information theory, inference and learning algorithms*. Cambridge university press.
- Magnusson, M., Andersen, M. R., Jonasson, J., and Vehtari, A. (2019). Bayesian leave-one-out cross-validation for large data. *Proceedings of the 36 International Conference on Machine Learning*, PMLR 97:4244–4253.
- Owen, A. B. (2013). Monte Carlo theory, methods and examples. Online book at <http://statweb.stanford.edu/~owen/mc/>, accessed 2017-09-09.
- Paananen, T., Piironen, J., Bürkner, P.-C., and Vehtari, A. (2019). Pushing the limits of importance sampling through iterative moment matching. *arXiv preprint 1906.08850*.
- Peruggia, M. (1997). On the variability of case-deletion importance sampling weights in the Bayesian linear model. *Journal of the American Statistical Association*, 92(437):199–207.
- Pickands, J. (1975). Statistical inference using extreme order statistics. *Annals of Statistics*, 3:119–131.
- Riihimäki, J. and Vehtari, A. (2014). Laplace approximation for logistic Gaussian process density estimation and regression. *Bayesian Analysis*, 9(2):425–448.
- Robert, C. P. and Casella, G. (2004). *Monte Carlo Statistical Methods, second edition*. Springer.
- Rychlik, T. (1994). Distributions and expectations of order statistics for possibly dependent random variables. *Journal of multivariate analysis*, 48(1):31–42.

- Sanz-Alonso, D. (2018). Importance sampling and necessary sample size: An information theory approach. *SIAM/ASA Journal on Uncertainty Quantification*, 6(2):867–879.
- Scarrot, C. and MacDonald, A. (2012). A review of extreme value threshold estimation and uncertainty quantification. *REVSTAT – Statistical Journal*, 10(1):33–60.
- Sen, P. K. (1959). On the moments of the sample quantiles. *Calcutta Statistical Association Bulletin*, 9(1-2):1–19.
- Stan Development Team (2017). *Stan modeling language: User’s guide and reference manual*. Version 2.16.0, <https://mc-stan.org/>.
- Vanhatalo, J., Riihimäki, J., Hartikainen, J., Jylänki, P., Tolvanen, V., and Vehtari, A. (2013). GPstuff: Bayesian modeling with Gaussian processes. *Journal of Machine Learning Research*, 14:1175–1179.
- Vehtari, A., Gabry, J., Yao, Y., and Gelman, A. (2018). loo: Efficient leave-one-out cross-validation and WAIC for Bayesian models, R package version 2.0.0.
- Vehtari, A., Gelman, A., and Gabry, J. (2017). Practical Bayesian model evaluation using leave-one-out cross-validation and WAIC. *Statistics and Computing*, 27(5):1413–1432.
- Vehtari, A., Gelman, A., Simpson, D., Carpenter, B., and Bürkner, P.-C. (2019). Rank-normalization, folding, and localization: An improved \hat{R} for assessing convergence of MCMC. *arXiv preprint arXiv:1903.08008*.
- Villani, M. and Larsson, R. (2006). The multivariate split normal distribution and asymmetric principal components analysis. *Communications in Statistics: Theory & Methods*, 35(6):1123–1140.
- Weber, S., Gelman, A., Carpenter, B., Lee, D., Betancourt, M., Vehtari, A., and Racine, A. (2016). Hierarchical expectation propagation for Bayesian aggregation of average data. *arXiv:1602.02055*.
- Yao, Y., Vehtari, A., Simpson, D., and Gelman, A. (2018). Yes, but did it work?: Evaluating variational inference. *Proceedings of the 35th International Conference on Machine Learning*, PMLR 80:5581–5590.
- Zhang, J. and Stephens, M. A. (2009). A new and efficient estimation method for the generalized Pareto distribution. *Technometrics*, 51(3):316–325.

A. Proofs

An important quantity in the proofs is $\xi_M = R^{-1}(1 - M/S)$. The following lemma shows how this grows with S if R has Pareto tails.

Lemma 1. *If $R(z) = 1 - cz^{-1/k'} + o(z^{-1/k'})$ for some $k' > 0$, then if $M = \mathcal{O}(S^{1/2})$ then $\xi_M = \mathcal{O}(S^{k'/2})$.*

Proof. The result follows from noting that

$$\begin{aligned} R(R^{-1}(1 - S^{-1/2})) &= 1 - S^{-1/2} \\ (R^{-1}(1 - S^{-1/2}))^{-1/k'} &= \frac{1}{c}S^{-1/2} + o\left(R^{-1}(1 - S^{-1/2})^{-1/k'}\right) \\ (R^{-1}(1 - S^{-1/2})) &= c^{k'}S^{k'/2} + o(S^{k'/2}). \end{aligned}$$

□

A.1. Proof of Theorem 1

It is sufficient to consider $h(\theta) \geq 0$.

$$\begin{aligned} I_h^S &= \frac{1}{S} \sum_{s=1}^S (r(\theta_s) \wedge r_{(S-M+1):S}) h(\theta_s) + \frac{1}{S} \sum_{j=1}^M \tilde{w}_j h(\theta_{S-M+j}) \\ &= \frac{1}{S} \sum_{s=1}^{S-M} r(\theta_s) h(\theta_s) + \rho_1 + \rho_2 + \rho_3, \end{aligned} \tag{9}$$

where the remainder terms are $\rho_1 = S^{-1}(r_{(S-M+1):S} + \tilde{w}_1)h(\theta_{S-M+1})$, $\rho_2 = \frac{r_{(S-M+1):S}}{S} \sum_{s=S-M+2}^S h(\theta_s)$, and $\rho_3 = \frac{1}{S} \sum_{j=2}^M \tilde{w}_j h(\theta_{S-M+j})$.

Conditional on the value of the order statistic, the expectation of the first term in (9) is

$$\mathbb{E} \left[\frac{1}{S} \sum_{s=1}^{S-M} r(\theta_s) h(\theta_s) \mid r_{(S-M+1):S} = U \right] = \frac{S-M}{SR(U)} \int_{r(\theta) < U} h(\theta) p(\theta) d\theta,$$

where the $R(U)$ in the denominator comes from the truncation of the distribution for $r(\theta)$. It follows that

$$\mathbb{E} \left[\frac{1}{S} \sum_{s=1}^{S-M} r(\theta_s) h(\theta_s) - I_h \right] = (1 - S^{-1/2}) \mathbb{E} \left[\frac{e(r_{S-M+1:S})}{R(r_{S-M+1:S})} \right].$$

Under condition A1, Theorem 2.1 of Gather and Tomkins (1995) shows that $r_{(S-M+1):S}$ converges in probability to ξ_M , so by A2, Lemma 1, and the continuous mapping theorem it follows that $e(r_{S-M+1:S}) \xrightarrow{P} e(\xi_M)(1 - S^{-1/2})^{-1} \rightarrow 0$. Noting that the sequence of random variables $e(r_{S-M+1:S})$ is non-negative and uniformly bounded, and hence uniformly integrable, it follows that $\mathbb{E}[e(r_{S-M+1:S})] \rightarrow 0$.

It remains to show that all of the remainder terms in (9) have expectations that converge to zero. Firstly, by condition A3

$$\begin{aligned} \mathbb{E}(\rho_1) &= S^{-1} \mathbb{E}[\mathbb{E}((r_{S-M+1:S} + \tilde{w}_1)h(\theta_{S-M+1}) \mid r_{S-M+1:S})] \\ &= S^{-1} \mathbb{E}[(r_{S-M+1:S} + \tilde{w}_1)m_1(r_{S-M+1:S})] \rightarrow 0. \end{aligned}$$

To bound $\mathbb{E}(\rho_2)$, we note that

$$\mathbb{E}(\rho_2 \mid r_{S-M+1:S} = U) = \frac{M-1}{S} U \int_{r(\theta) > U} h(\theta) g(\theta) d\theta.$$

From (A4) it follows that $\mathbb{E}(\rho_2 \mid r_{S-M+1:S} = U) = (M-1)S^{-1}o(U)$, and hence $\mathbb{E}(\rho_2) \rightarrow 0$ by Lemma 1. By a similar argument, condition (A4) and Lemma 1 implies $\mathbb{E}(\rho_3) \rightarrow 0$.

A.2. Proof of Theorem 2

We write

$$I_h^S = \rho_0 + \rho_1 + \rho_2 + \rho_3,$$

where $\rho_0 = S^{-1} \sum_{s=1}^{S-M} r(\theta_s) h(\theta_s)$ and the other terms are defined as they were in the proof of Theorem 1. We begin considering the event $A = \{r_{S-M+1:S} = U, h(\theta_{S-M+1:S}) = H\}$ and noting,

$$\text{Var}(I_h^S) = \text{Var}(\mathbb{E}(I_h^S \mid A)) + \mathbb{E}(\text{Var}(I_h^S \mid A)).$$

From above, we know that

$$\text{Var}(\mathbb{E}(\rho_0 \mid A)) = \frac{S-M}{S^2} \text{Var}(r_{S-M+1:S} e(r_{S-M+1:S})) \leq o(1).$$

For $\text{Var}(\rho_1)$, $S^2 \mathbb{E}(\rho_1^2) \leq \mathbb{E}[(r_{S-M+1:S}^2 + \tilde{w}_1^2) m_2(r_{S-M+1:S}) + 2r_{S-M+1:S} m_1(r_{S-M+1:S})]$, which is finite by assumption (B2).

From above, we know that

$$\text{Var}(\mathbb{E}(\rho_2 \mid A)) \leq \left(\frac{M-1}{S}\right)^2 \mathbb{E}_g(|h(\theta)|)^2 \text{Var}(r_{S-M+1:S}),$$

which goes to zero.

Bounding \tilde{w}_j above, we see that

$$\text{Var}(\mathbb{E}(\rho_3 \mid A)) \leq \mathbb{E}_g(|h(\theta)|)^2 S^{k+1-2} = o(1).$$

A quick examination shows that $\text{Cov}(\mathbb{E}\rho_i, \mathbb{E}\rho_j)$ goes to zero for all $i \neq j$ if

$$\mathbb{E}(r_{S-M+1:S}^2 m_1(r_{S-M+1:S})) = o(S^2),$$

which holds by assumption (B2).

This completes the proof that $\text{Var}(\mathbb{E}(I_h^S \mid A)) = o(1)$.

To show that $\mathbb{E}(\text{Var}(\rho_j \mid A)) \rightarrow 0$ for $j = 0, 2, 3$, we first show that $\mathbb{E}(\rho_j^2) \rightarrow 0$. We will complete the proof by showing that $\mathbb{E}(\mathbb{E}(\rho_j \mid A)^2) \rightarrow 0$ for $j = 0, 2, 3$.

First we will derive an expression for $\mathbb{E}(\rho_0^2)$. Conditioning on A , it follows that

$$\begin{aligned} S^2 \mathbb{E}(\rho^2 \mid A) &= \sum_{s=1}^{S-M} \mathbb{E}(r(\theta_s)^2 h(\theta_s)^2 \mid A) \\ &= (S-M) \int_{r(\theta) < U} r(\theta) h(\theta)^2 f(\theta) d\theta \\ &\leq (S-M) U \mathbb{E}_f(h(\theta)^2). \end{aligned}$$

Noting that $\mathbb{E}(S^{-1} r_{S-M+1:S}) \leq \mathbb{E}(S^{-1} r_{S:S}) \leq \mathbb{E}(R)$, it follows that $\mathbb{E}(\rho_0^2)$ is finite.

To show that $\mathbb{E}(\rho_0^2) \rightarrow 0$, we note that $\mathbb{E}(R^{1+\delta}) < \infty$ implies $\mathbb{E}(r_{S-M+1:S}^{1+\delta})$ is uniformly bounded and hence $r_{S-M+1:S}$ is uniformly integrable. Under the von Mises condition (B1), Theorem 10.8.1 of David and Nagaraja (2003) shows that $r_{S-M+1:S}$ is asymptotically normal with mean ξ_M and hence $\mathbb{E}(r_{S-M+1:S}) \rightarrow \xi_M$. We will show that $\xi_M = O(S^{k'/2})$ and hence $\mathbb{E}(\rho_0^2) \leq \mathcal{O}(S^{k'/2-1}) = o(S^{-1/2})$.

To bound $\mathbb{E}(\rho_2^2)$, we note that, conditional on the event $\{r_{S-M+1:S} = U\}$, $h(\theta_s)$ are conditionally independent draws from $h(\theta)$, where $\theta \sim p(\theta \mid r(\theta) > U)$. It follows that

$$S^2 \mathbb{E}(\rho_2^2 \mid r_{S-M+1:S} = U) = U^2(M-1) \int_{r(\theta) > U} h(\theta)^2 g(\theta) d\theta \leq (M-1)U^2 \mathbb{E}_g(h^2(\theta))$$

which goes to zero by (B3).

Following similar reasoning, we get $\mathbb{E}(\rho_3^2) \leq S^{-2} \mathbb{E}_g(h^2(\theta)) \sum_{j=2}^M \tilde{w}_j \leq S^{k/2-2} \mathbb{E}_g(h^2(\theta))$, which goes to zero by (B3).

To complete the proof we need to show that $\mathbb{E}(\text{Cov}(\rho_i, \rho_j \mid A))$ goes to zero. Enumerating all of the crossproducts, they are bounded in absolute value by terms that we have shown to go to zero. (In the interest of space, we will not list all six combinations.) Hence $\mathbb{E}(\text{Var}(I_h^S \mid A)) = o(1)$, which completes the proof.

B. Simulated examples

In the following simulated examples we know the true target value and vary the proposal distribution. This allows us to study how \hat{k} functions as a diagnostic and how bad the approximating distribution has to be before the importance sampling estimates break down. To diagnose the performance with respect to the number of draws S , in each of the examples we vary the number of draws from $S = 10^2$ to $S = 10^5$. We examine the estimates for the normalization term (0th moment), which also has a special role later in importance sampling examples, and estimates for $\mathbb{E}[h(\theta)]$, where $h(\theta) = \theta$ (1st moment) or $h(\theta) = \theta^2$ (2nd moment). Although in these examples the normalization terms of both p and g are available, all experiments have been made assuming that normalization terms are unknown and self-normalized importance sampling is used.

B.1. Exponential target and proposal

In the first simulated example the target and proposal distributions are exponential distributions with scale parameter 1 and $1/\theta$, respectively. In this case, it is possible to compute the distribution of the importance ratios in closed form. The variance is infinite when $\theta > 2$ (Robert and Casella, 2004), and we know that the distribution of the importance ratios has the form of a generalized Pareto distribution.

Figure 9 shows 100 simulations of estimating the normalization term using a proposal distribution with scale parameter $1/3$, leading to $k \approx 0.66$ which illustrates the typical behavior of IS, TIS and PSIS when $0.5 < k < 0.7$. IS has high variability, while TIS and PSIS produce more stable estimates. For the same 100 simulations, Figure 9 shows the 100 largest IS raw ratios and modified weights from TIS, PSIS and PSISa. PSISa uses all the raw ratios, that is $M = S$, to fit the generalized Pareto distribution and estimate \hat{k} . IS has high variability, TIS truncates the largest weights downwards, while PSIS reduces the variability without biasing the largest weights. PSISa uses more draws to estimate \hat{k} and has smaller variability than PSIS.

Figure 10 shows the bias and standard deviation of the 0th, 1st, and 2nd moment estimates with respect to the number of draws S computed from 1000 simulations. This illustrates the

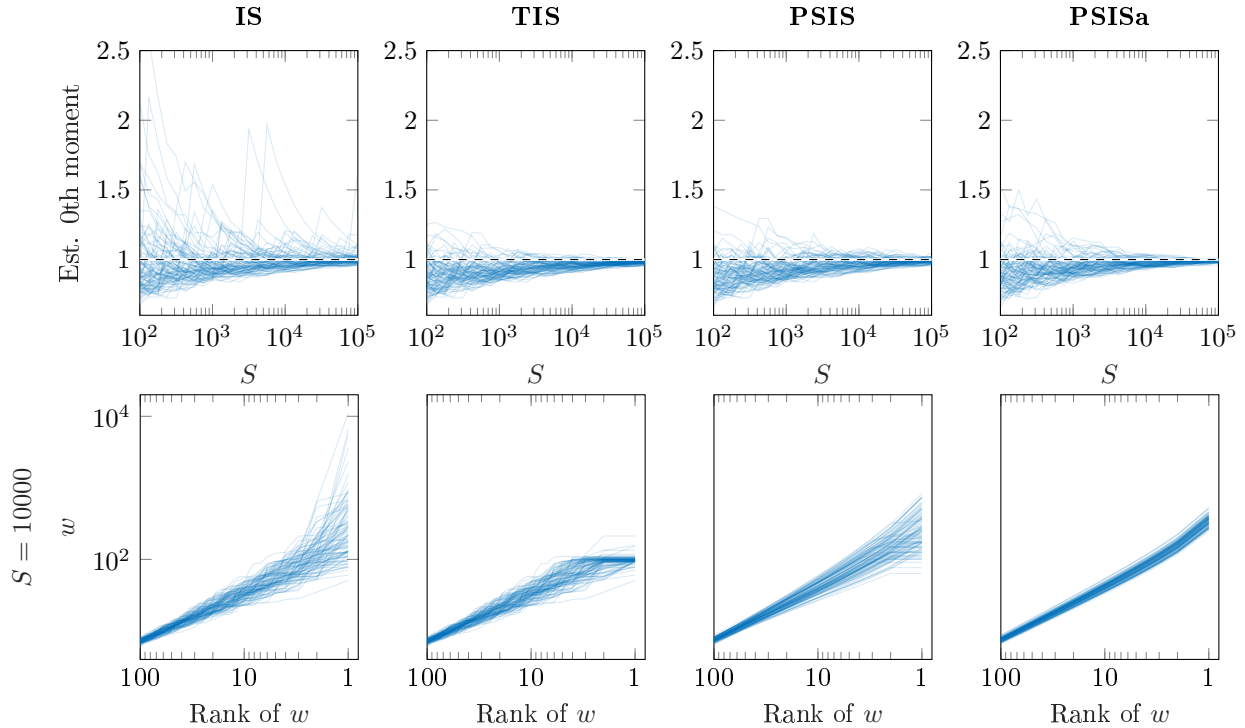


Figure 9: Each graph has 100 blue lines, and each line is the trajectory of the estimated normalization term using different initial random seeds. The first line shows the bias and variance of the different estimators when $h(\theta) = 1$ as the MCMC sample size increases. The second line shows the distribution of the importance sampling weights when $S = 10000$. The target and proposal distributions are exponential distributions with mean parameters 1 and 13 respectively and the distribution of ratios does not have finite variance.

typical differences between the methods. IS (yellow) has the smallest bias but the largest deviation. PSISa (dashed blue) has the smallest deviation, and similar bias as PSIS. TIS (red) has the largest bias and with large S similar deviation as PSISa. PSIS (solid blue) has similar bias as PSISa, but slightly larger deviation than PSISa.

Figures 11, 12, and 13 show the RMSE and mean of the Monte Carlo error estimates for 0th, 1st and 2nd moment estimates with varying $\theta \in (1.3, 1.5, 2, 3, 4, 10)$. We can see that convergence rate depends *continuously* on k . There is no abrupt jump at $k = \frac{1}{2}$. The results for the 1st and 2nd moment agree well with the theoretical results by Epifani et al. (2008), that is, the conditions for the existence of the moments of the distribution of $r(\theta)$ and $h(\theta)r(\theta)$. Simulations suggest that similar results would be obtained with $h(\theta)$ corresponding to higher moments. All methods have impractical convergence rates in the case of larger k . With smaller k values the errors are similar, but already at the borderline case $k = \frac{1}{2}$ IS has larger RMSE. TIS has larger RMSE than PSIS and PSISa for large k values. There is not much difference in RMSE between PSIS and PSISa, demonstrating the diminishing benefit of using a larger sample to estimate k . The Monte Carlo error estimates are unbiased for IS, but have high variance for larger k (not shown here). The Monte Carlo error estimates are unbiased for TIS when $k < \frac{1}{2}$, but the error is underestimated for $k > \frac{1}{2}$. The Monte Carlo estimates for PSIS and PSISa are useful for $k \lesssim 0.7$, with PSISa yielding slightly more accurate error estimates. The results from PSISa show that using larger M (in PSISa $M = S$) would give better estimates, but this works only if the M largest weights are well approximated by the generalized Pareto distribution. For easier comparison of RMSEs between IS, TIS and PSIS, Figure 1 shows the relative RMSEs.

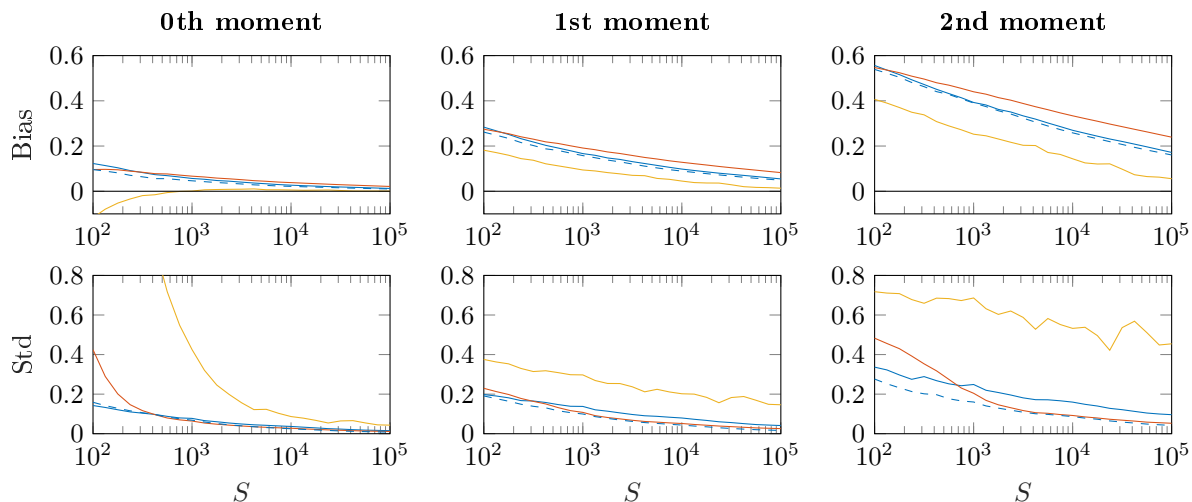


Figure 10: *Bias and standard deviation of the 0th, 1st, and 2nd moment estimates with respect to the number of draws S computed from 1000 simulations. Target and proposal distributions are exponential distributions with scale parameters 1 and $1/3$ respectively, leading to $k \approx 0.66$. IS is yellow, TIS is red, PSIS is blue and PSISa is blue dashed.*

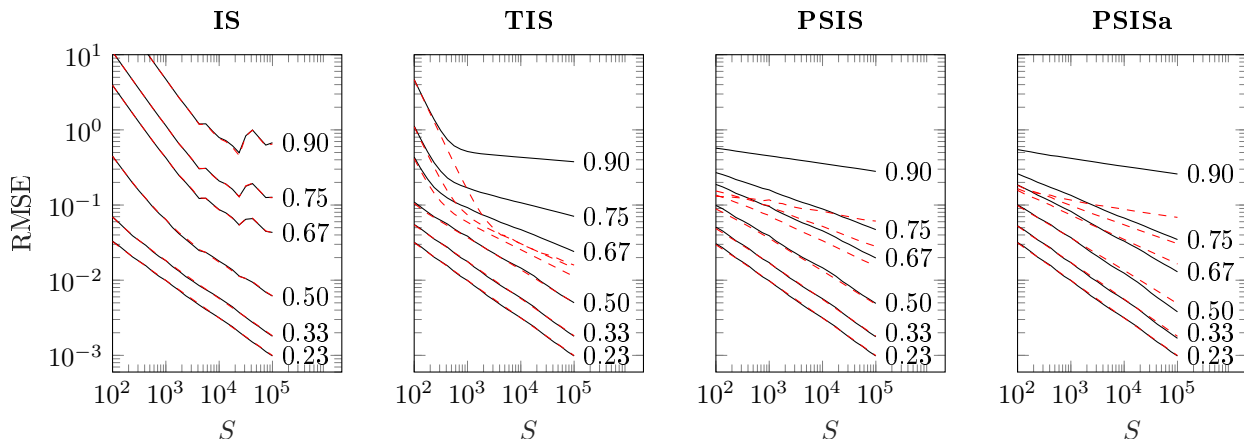


Figure 11: *RMSE (black) and the mean of the Monte Carlo error estimates (red dashed) for the 0th moment estimate. Target and proposal distributions are exponential distributions with scale parameters 1 and $1/\theta$ respectively, with $\theta \in (1.3, 1.5, 2, 3, 4, 10)$. The numbers at the end of black lines are average of \hat{k} values estimated when $S = 10^5$.*

Figure 14 shows how the practical convergence rate depends on h specific \hat{k} estimates. For direct independent draws from $p(\theta)$ the variance of the Monte Carlo would decrease as S^{-1} . For PSIS we observe convergence rates $S^{-\alpha}$, where $0 < \alpha \leq 1$ depends on k and can be estimated from \hat{k} . Here \hat{k} is estimated using the mean from 1000 simulations, with $S = 10^5$ for each simulation. Convergence rates are estimated by a linear fit to the RMSE results illustrated in Figures 11, 12, 13. Previously in the literature the focus has been mostly on the binary decision between $k < \frac{1}{2}$ and $k \geq \frac{1}{2}$, although the Berry-Esseen theorem states that the convergence rate to normality is faster with decreasing k . Here we can see that in practice the convergence rate starts to decrease for PSIS when $k > \frac{1}{4}$ and for PSISa when $k > \frac{1}{3}$. In this and the other experiments in the paper the convergence rate at $k = \frac{1}{2}$ is approximately with $\alpha \approx 0.87$, and at $k = 0.7$ is approximately with $\alpha \approx 0.6$ (marked in

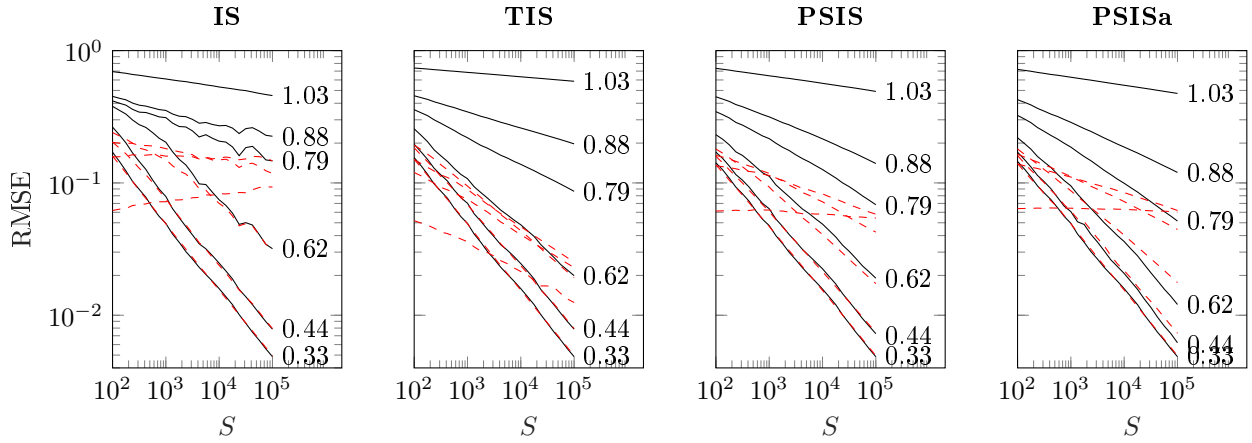


Figure 12: *RMSE (black) and the mean of the Monte Carlo error estimates (red dashed) for the 1st moment estimate. Target and proposal distributions are exponential distributions with scale parameters 1 and $1/\theta$ respectively, with $\theta \in (1.3, 1.5, 2, 3, 4, 10)$. For each graph, the lines are ordered with low values of theta at bottom and high values at top, with high θ values leading to high RMSE and high \hat{k} . The numbers at the end of black lines are average of h specific \hat{k} values estimated when $S = 10^5$.*

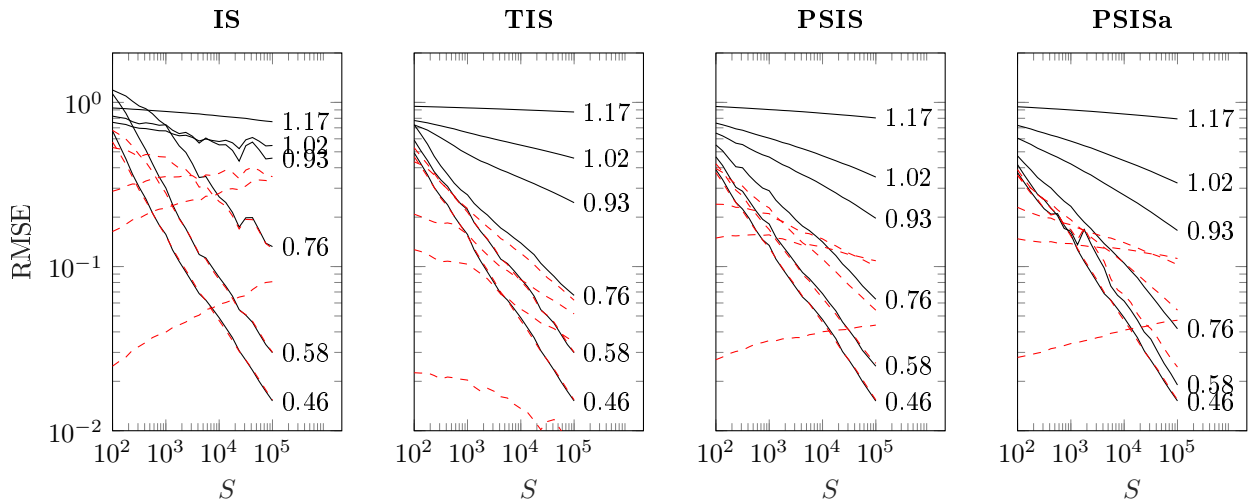


Figure 13: *RMSE (black) and the mean of the Monte Carlo error estimates (red dashed) for the 2nd moment estimate. Target and proposal distributions are exponential distributions with scale parameters 1 and $1/\theta$ respectively, with $\theta \in (1.3, 1.5, 2, 3, 4, 10)$. For each graph, the lines are ordered with low values of theta at bottom and high values at top, with high θ values leading to high RMSE and high \hat{k} . The numbers at the end of black lines are average of h specific \hat{k} values estimated when $S = 10^5$.*

the plots). In this experiment we added results for $\theta \in (1.9, 2.1)$ which have k just below and above 0.5, illustrating that there is no sharp transition. A dashed line has been drawn from $k = 0.5, \alpha = 1$ to $k = 0, \alpha = 0$, which matches well the observed behavior. Based on analytic consideration we assume that h specific \hat{k} for $\sqrt{1 + h(\theta)^2}r(\theta)$ for the 1st and 2nd moment are not as accurate as \hat{k} estimates for the ratios $r(\theta)$ (0th moment). This is likely explanation why the corresponding empirical convergence rate curves go slightly beyond the above mentioned limit line. PSISa is able to produce better convergence rates, but the

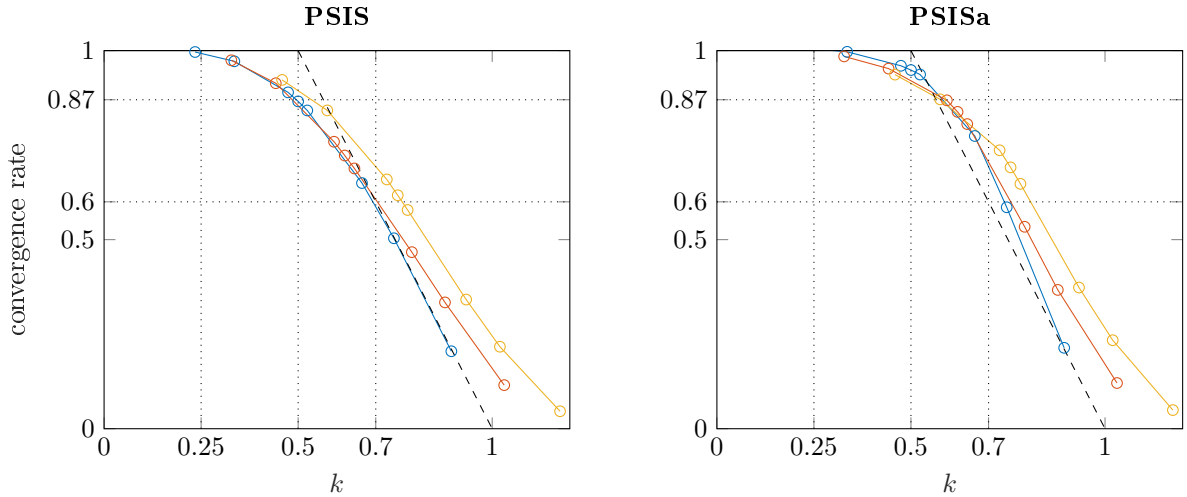


Figure 14: *The practical convergence rates for PSIS and PSISa estimating 0th (blue), 1st (red) and 2nd (yellow) moments. Target and proposal distributions are exponential distributions with scale parameters 1 and $1/\theta$ respectively, with $\theta \in (1.3, 1.5, 1.9, 2, 2.1, 3, 4, 10)$. The circles in each line correspond to the results with different θ , with higher θ values leading to lower convergence rates and higher \hat{k} values. \hat{k} estimates in case of 1st and 2nd moments are h specific. Dotted horizontal lines at 0.87 and 0.6 show the typical convergence rates at $\hat{k} = 0.5$ and $\hat{k} = 0.7$ for several different experiments in this paper.*

difference is small and PSISa using $M = S$ is not usually applicable.

B.2. Univariate normal and Student's t

The previous example with exponential target and proposal is especially suited for PSIS, as the whole importance ratio distribution is well fitted with the generalized Pareto distribution. In this section we consider various univariate target and proposal distribution combinations to show the behavior in the case of different target-proposal tail combinations. In the next section we examine the corresponding multivariate cases.

We do not use the simulated example by Ionides (2008) having the target $p(\theta) = N(\theta | 0, 1)$ and the proposal $g(\theta) = N(\theta | 0, \sigma)$, as both distributions have the same mean and thus when estimating the 1st moment the lowest RMSE would be obtained by using identity weights and $\sigma \rightarrow 0$.

To test the performance for the 0th, 1st and 2nd moments we choose the proposal distributions to have different mean and scale than the target distribution. The tested pairs are

1. $p(\theta) = N(0, 1)$, $g(\theta) = N(\mu, 0.8)$: This is a special case with the matching tail shape of the target and proposal leading to a case which is favorable for PSIS.
2. $p(\theta) = t_{20}(0, 1)$, $g(\theta) = N(\mu, 0.9)$: This resembles an applied case of using a Gaussian posterior approximation when the target has a thicker tail.
3. $p(\theta) = t_{20}(0, 1)$, $g(\theta) = t_{21}(\mu, 0.8)$: This resembles an applied case of leave-one-out importance sampling where the proposal has a slightly thinner tail.
4. $p(\theta) = t_7(0, 1)$, $g(\theta) = t_8(\mu, 0.8)$: This resembles an applied case of leave-one-out importance sampling where the proposal has a slightly thinner tail, but both having thicker tails than in case 3.

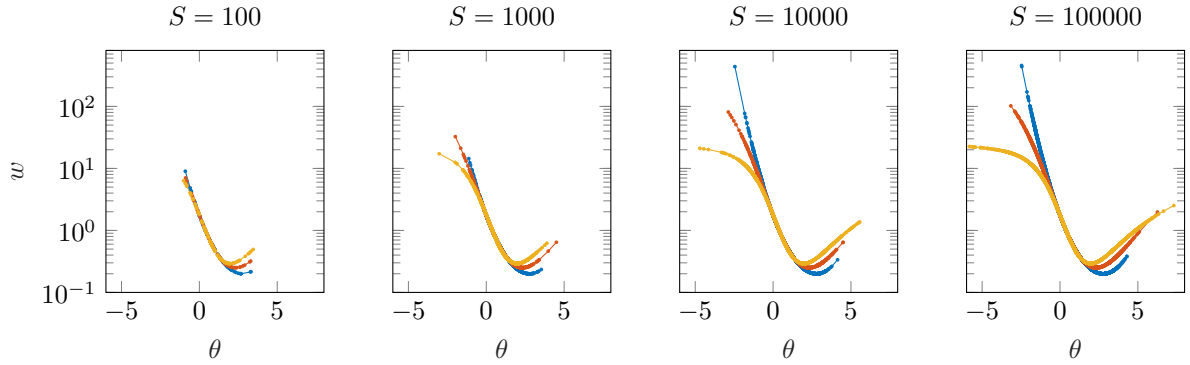


Figure 15: *Plain IS weights plotted by θ for different target-proposal pairs: $p(\theta) = N(0, 1)$, $g(\theta) = N(1.5, 0.8)$ (blue), $p(\theta) = t_{20}(0, 1)$, $g(\theta) = t_{21}(1.5, 0.8)$ (red), $p(\theta) = t_7(0, 1)$, $g(\theta) = t_8(1.5, 0.8)$ (yellow), and different sample sizes S .*

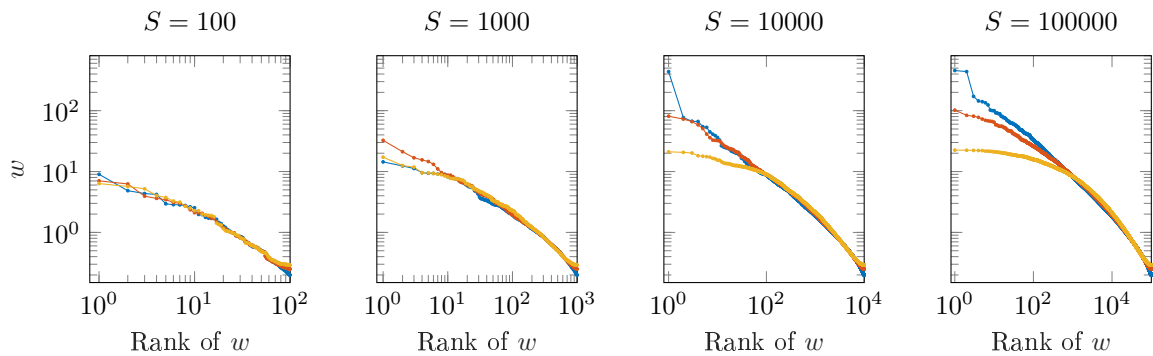


Figure 16: *Sorted plain IS weights plotted by rank for different target-proposal pairs: $p(\theta) = N(0, 1)$, $g(\theta) = N(1.5, 0.8)$ (blue), $p(\theta) = t_{20}(0, 1)$, $g(\theta) = t_{21}(1.5, 0.8)$ (red), $p(\theta) = t_7(0, 1)$, $g(\theta) = t_8(1.5, 0.8)$ (yellow), and different sample sizes S .*

Here we have left out easy examples where the proposal would have a thicker tail than the target. To vary how well the proposal matches the target, the mean of the proposal μ is varied.

Figure 15 shows plain IS weights for different θ , different target-proposal pairs (1, 3 and 4 in the above list with $\mu = 1.5$), and different sample sizes S . With increasing sample size S we get more draws from the tails and the differences between the weight functions become more apparent. To better illustrate how the tail shape of the empirical weight distributions change when the sample size S increases, Figure 16 shows the same weights sorted and plotted by rank. With $S = 100$ the weight distributions look similar and the corresponding \hat{k} 's are 0.66, 0.66, and 0.64. As S increases the distributions of the weights eventually look different and the corresponding \hat{k} 's are 0.66, 0.47, and -0.28 . This shows that using only a small portion of the raw weights in the tail allows the \hat{k} diagnostic to adapt to the empirically observed tail shape. Figure 16 also illustrates the motivation to truncate the weights at the maximum raw weight value $\max(r_s)$. This will allow the use of larger M for the Pareto fit to reduce the variance, while being able to adapt when the magnitude of the weights is saturating with increasing S .

Based on the above \hat{k} values we may assume that PSIS is beneficial for small S , and for cases 3 and 4 when S grows eventually plain IS will also work well. Figure 17 shows the mean RMSE from 1000 simulations for the four different target-proposal pairs as listed above with

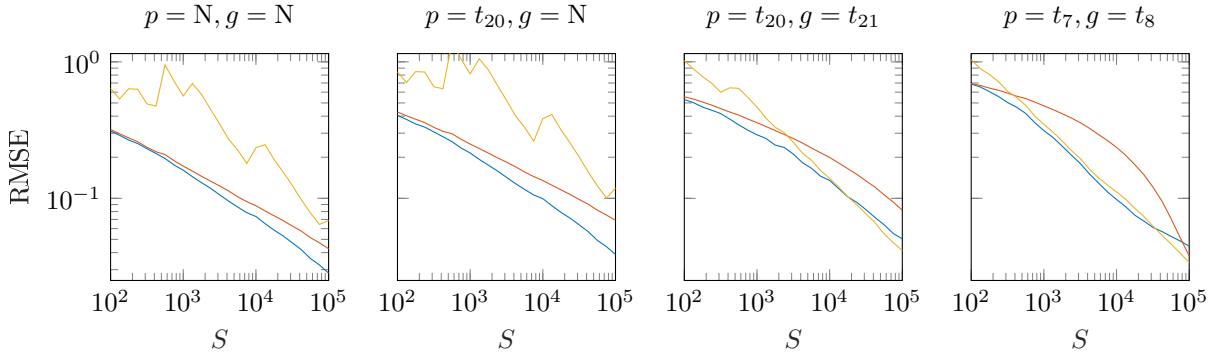


Figure 17: The mean RMSE from thousand simulations for the different target-proposal pairs with μ from left to right being 1.5, 2, 2.25, and 3. IS is yellow, TIS is red and PSIS is blue.

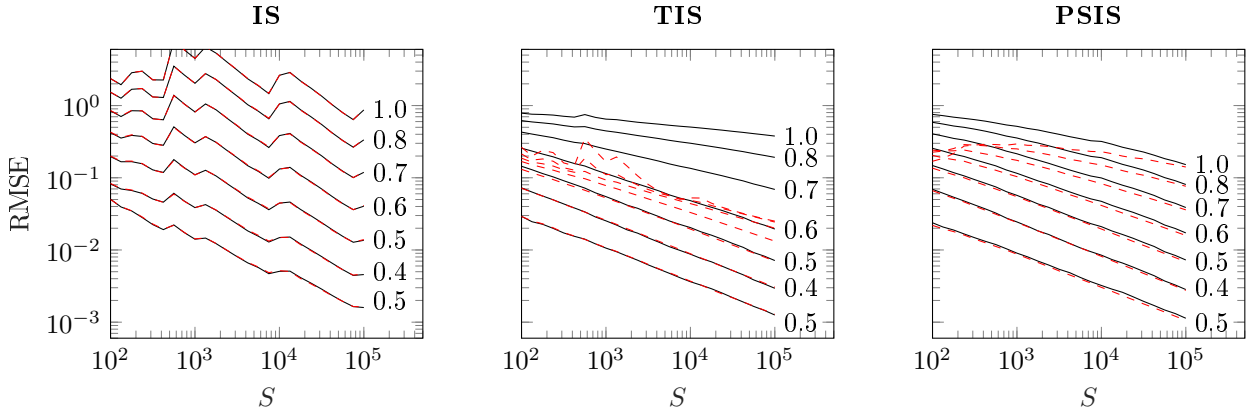


Figure 18: RMSE (black) and the mean of the Monte Carlo error estimates (red dashed) for the 0th moment estimate. The target distribution is $t_{20}(0, 1)$ and the proposal distribution is $N(\mu, 0.9)$, with $\mu \in (0, 0.5, 1.0, 1.5, 2.0, 2.5, 3.0)$. For each graph, the lines are ordered with low values of θ at bottom and high values at top, with high θ values leading to high RMSE and high \hat{k} . The numbers at the end of black lines are average of \hat{k} values estimated when $S = 10^5$.

hand-picked μ values to illustrate the typical behavior of IS, TIS and PSIS when $0.5 \geq \hat{k} < 0.7$ (for very low \hat{k} there are no differences and for very high values all methods fail). PSIS is able to adapt well in all cases and has the smallest RMSE in almost all cases. When the proposal distribution has a thin tail (e.g. the normal in cases 1 and 2), IS has high variance and the variance remains high with increasing S . If the tail of the proposal is thick (e.g. Student's t) and asymptotically the weight distribution has a short tail (small k), PSIS performs better than IS for small S . Eventually the RMSE of IS can get as small as the RMSE of PSIS. Most of the time TIS has a larger RMSE than PSIS. For thick tailed proposals TIS is not able to adapt well to the changing shape of the empirical weight distribution.

Figure 18 shows as a representative example of the RMSE and Monte Carlo error estimates for 0th moment estimated with IS, TIS and PSIS in case of $p(\theta) = t_{20}(0, 1)$, $g(\theta) = N(\mu, 0.9)$. PSIS is more stable, has smaller RMSE than IS, and has more accurate Monte Carlo error estimates than TIS.

Figure 19 shows the practical convergence rate with respect to h specific \hat{k} estimates. We observe similar behavior as in in the exponential distribution example. For thick tail proposal distributions we tend to overestimate \hat{k} values more than for the thin tailed proposal

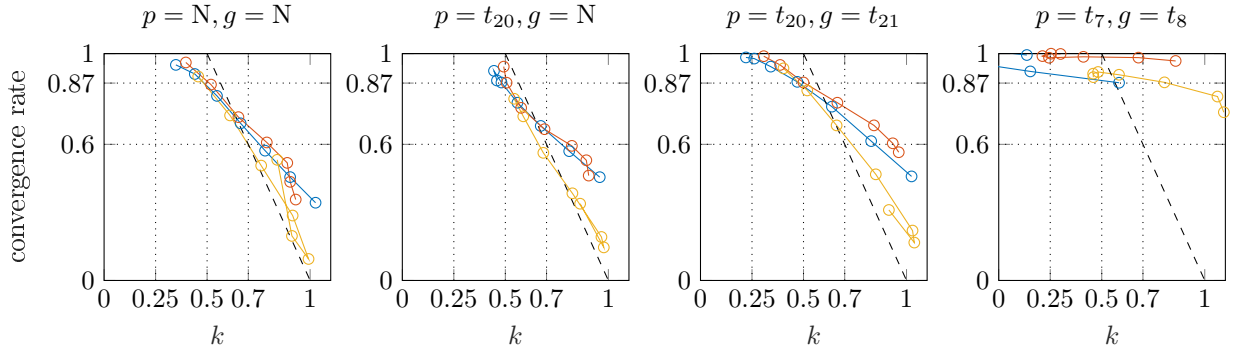


Figure 19: *The practical convergence rates for PSIS estimating 0th (blue), 1st (red) and 2nd (yellow) moments. Different target-proposal distribution pairs are used in different subplots. \hat{k} estimates in case of 1st and 2nd moments are h specific. Dotted horizontal lines at 0.87 and 0.6 show the typical convergence rates at $\hat{k} = 0.5$ and $\hat{k} = 0.7$ for several different experiments in this paper.*

distributions, but the convergence rates stay good. Given estimated \hat{k} values, we can use the dashed diagonal line drawn from $k = 0.5, \alpha = 1$ to $k = 0, \alpha = 0$ to provide a conservative convergence rate estimate.

B.3. Multivariate normal and Student's t

In this section we consider the isotropic multivariate versions of the four target-proposal pairs as the number of dimensions increases. In addition, we also examine a case where the proposal has thicker tails than the target, and show that with an increasing number of dimensions this will also lead to increasing variability of the weights. The compared target-proposal pairs are

1. $p(\theta) = N(\mathbf{0}, I), g(\theta) = N(0.4 \cdot \mathbf{1}, 0.8I)$
2. $p(\theta) = t_{20}(\mathbf{0}, I), g(\theta) = N(0.4 \cdot \mathbf{1}, 0.9I)$
3. $p(\theta) = t_{20}(\mathbf{0}, I), g(\theta) = t_{21}(0.4 \cdot \mathbf{1}, 0.8I)$
4. $p(\theta) = t_7(\mathbf{0}, I), g(\theta) = t_8(0.4 \cdot \mathbf{1}, 0.8I)$
5. $p(\theta) = N(\mathbf{0}, I), g(\theta) = t_7(0.4 \cdot \mathbf{1}, 0.8I)$

In all of these cases, the proposal distribution is just slightly displaced and with slightly narrower scale. The 5th proposal distribution has thicker tails than the target distribution, so that the importance ratios are bounded and thus have finite variance. The number of dimensions is varied as $D \in (1, 2, 4, 8, 16, 32, 64)$.

Figure 20 shows the mean RMSE from 1000 simulations for the five different target-proposal pairs as listed above with $D = 16$ for all except the last case with $D = 32$. The plots illustrate the typical behavior of IS, TIS and PSIS when $0.5 \leq \hat{k} < 0.7$ (for very small \hat{k} there are no differences and for very high values all methods fail). PSIS has the smallest RMSE in all cases. TIS has a slower convergence rate than PSIS. IS is overall more unstable and has higher RMSE. Comparing the case with a thick tailed proposal distribution to the corresponding univariate case we see that IS requires larger S before beginning to stabilize. The rightmost subplot illustrates that even if the proposal distribution has thicker tails than the target distribution and the importance ratios are bounded, the variance of the importance

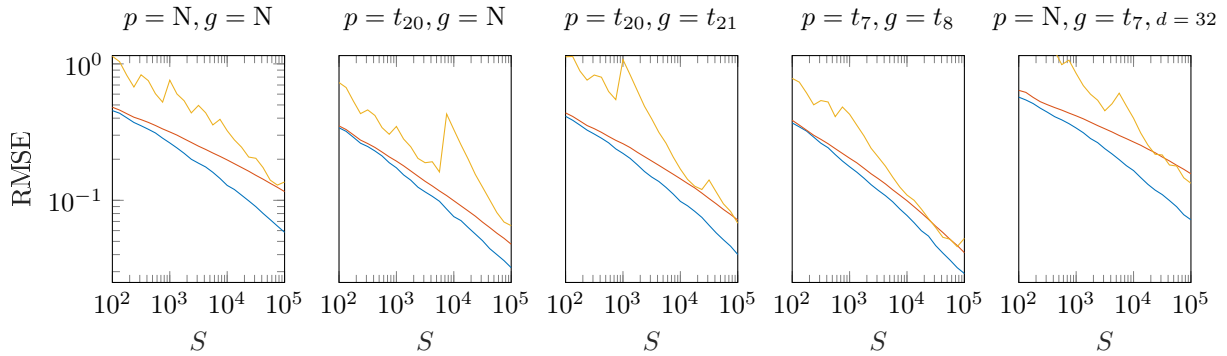


Figure 20: The mean RMSE from 1000 simulations for the different target-proposal pairs with $D = 16$ for all except the last one with $D = 32$. IS is yellow, TIS is red and PSIS is blue.

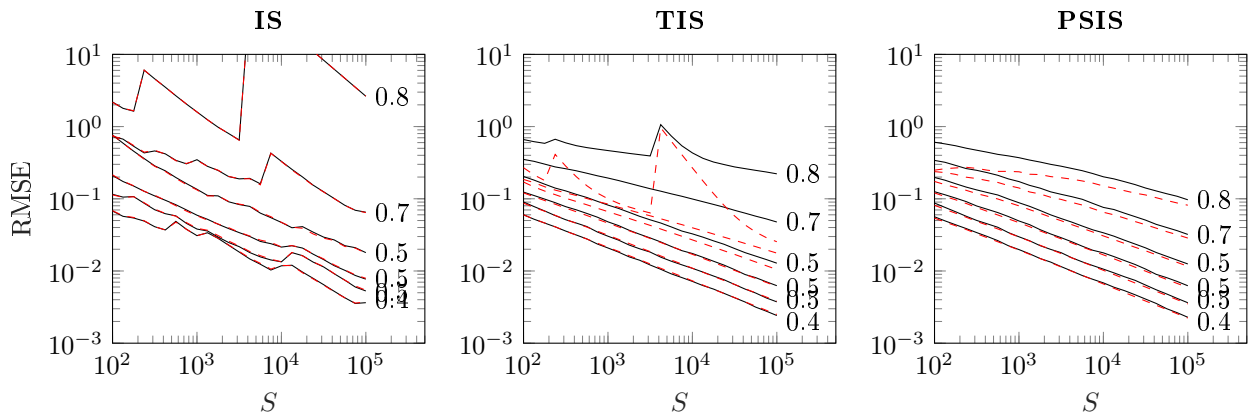


Figure 21: RMSE (black) and the mean of the Monte Carlo error estimates (red dashed) for the 0th moment estimate. The target distribution is $t_{20}(\mathbf{0}, I)$ and the proposal distribution is $N(0.41, 0.9I)$, with the number of dimensions $D \in (1, 2, 4, 8, 16, 32, 64)$. For each graph, the lines are ordered with low values of D at bottom and high values at top, with high D values leading to high RMSE and high \hat{k} . The numbers at the end of black lines are average of \hat{k} values estimated when $S = 10^5$.

ratio distribution can be high when the number of dimensions D , and IS is not a safe choice in finite sample case.

Figure 21 shows a representative example of the RMSE and Monte Carlo estimates for 0th moment estimated with IS, TIS and PSIS with $p(\theta) = t_{20}(\mathbf{0}, I)$, $g(\theta) = N(0.4 \cdot \mathbf{1}, 0.9I)$. PSIS is more stable, has smaller RMSE than IS and TIS, and has more accurate Monte Carlo estimates than TIS. All methods eventually fail as the number of dimensions increases and even a small difference in the distributions is amplified. Having a bounded importance ratios and thus finite variance, does not prevent the variance to be impractically high in finite sample case. In these multivariate examples, we observe sudden large jumps also for TIS. Truncation in TIS fails when there is one extremely large weight that causes the truncation level to rise so high that other large weights are not truncated. PSIS performs better in the same situation as one extreme large weight doesn't affect the generalized Pareto fit as much.

Figure 22 shows the practical convergence rate with respect to the h specific \hat{k} estimates. We observe similar behavior as in the univariate example. As we saw before, the observed convergence rate with respect to \hat{k} follows quite well the dashed diagonal line drawn from $k = 0.5, \alpha = 1$ to $k = 0, \alpha = 0$.

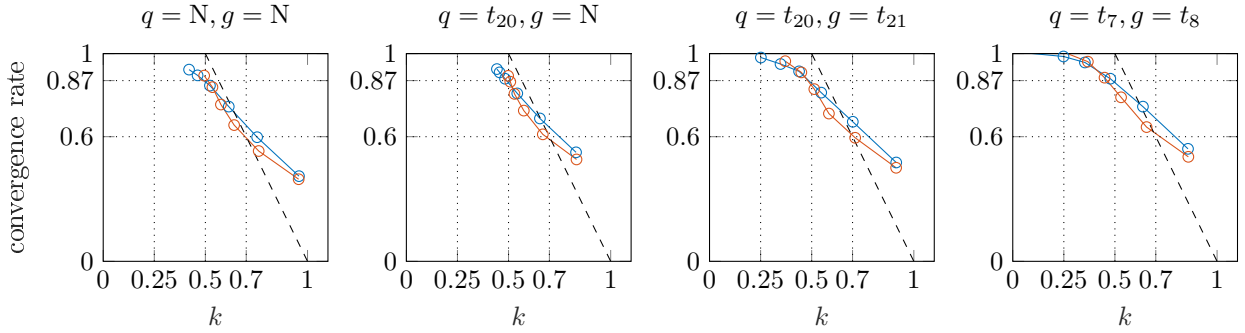


Figure 22: The practical convergence rates for PSIS estimating 0th (blue), 1st (red) and 2nd (yellow) moments. Different target-proposal distribution pairs are used in different subplots. \hat{k} estimates in case of 1st and 2nd moments are h specific. Dotted horizontal lines at 0.87 and 0.6 show the typical convergence rates at $\hat{k} = 0.5$ and $\hat{k} = 0.7$ for several different experiments in this paper.

C. Regularization of Pareto fit for small S

To reduce the variance of the \hat{k} estimate for small S (S less than about 1000), we use an additional regularization

$$\hat{k} = (M\hat{k} + 10 \cdot 0.5)/(M + 10),$$

which corresponds approximately to a weakly informative Gaussian prior that has a weight of 10 observations from the tail shrinking towards 0.5. If $S = 100$ and using the proposed rule to choose $M = 20$, we see that \hat{k} is strongly regularized. If $S = 1000$ and using the proposed rule to choose $M = 95$, we see that the regularization has only weight of one tenth of the data. We acknowledge that this regularization adds bias towards 0.5, but based on our simulation results, this reduced the variance and RMSE of the PSIS estimates with small S , without introducing significant bias or affecting the RMSE for larger S . In many applications we would assume $S > 1000$, but in sequential and iterative methods such as particle filters and black box variational inference we may want to use small S due to computational speed issues.

D. Adjusting M in case of dependent MCMC draws

We adjust the algorithm in the following way to take into account the usually smaller effective sample size of dependent MCMC draws. Due to correlated MCMC draws, we use more ratios in the tail to keep the variance of \hat{k} in control. We adjust the number of tail ratios used as $M = 3\sqrt{S/R_{\text{eff},\text{MCMC}}}$ if $S > 225$ or $M = S/5$ for lower values of S , where $R_{\text{eff},\text{MCMC}} = S_{\text{eff},\text{MCMC}}/S$ is the estimated relative efficiency of the MCMC draws, and the effective sample size $S_{\text{eff},\text{MCMC}}$ for $r(\theta)$ is computed using the split-chain effective sample size estimate method (Vehtari et al., 2019). This effective sample size is not directly the effective sample size for \hat{k} , but it is related and much easier to compute.

E. Stan Gaussian linear regression model for stack loss data

```
data {
  int<lower=0> N;
```

```

int<lower=0> p;
vector[N] y;
matrix[N,p] x;
}
// to standardize the x's
transformed data {
  matrix[N,p] z;
  vector[p] mean_x;
  vector[p] sd_x;
  real sd_y;
  sd_y <- sd(y);
  for (j in 1:p) {
    mean_x[j] = mean(col(x,j));
    sd_x[j] = sd(col(x,j));
    for (i in 1:N)
      z[i,j] = (x[i,j] - mean_x[j]) / sd_x[j];
  }
}
parameters {
  real beta0;
  vector[p] beta;
  real<lower=0> sigmasq;
  real<lower=0> phi;
}
transformed parameters {
  real<lower=0> sigma;
  vector[N] mu;
  sigma = sqrt(sigmasq);
  mu = beta0 + z * beta;
}
model {
  beta0 ~ normal(0, 100);
  phi ~ cauchy(0, sd_y);
  beta ~ normal(0, phi);
  sigmasq ~ inv_gamma(.1, .1);
  y ~ normal(mu, sigma);
}
generated quantities {
  vector[N] log_lik;
  for (i in 1:N)
    log_lik[i] = normal_lpdf(y[i] | mu[i], sigma);
}

```